

# Sensitivity and Nonlinearity of Thermoacoustic Oscillations

Matthew P. Juniper<sup>1</sup> and R.I. Sujith<sup>2</sup>

<sup>1</sup>Department of Engineering, University of Cambridge, Cambridge CB2 1PZ, United Kingdom; email: mpj1001@cam.ac.uk

<sup>2</sup>Department of Aerospace Engineering, Indian Institute of Technology Madras, Chennai 600036, India; email: sujith@iitm.ac.in

Annu. Rev. Fluid Mech. 2018. 50:661–89

First published as a Review in Advance on October 23, 2017

The *Annual Review of Fluid Mechanics* is online at [fluid.annualreviews.org](http://fluid.annualreviews.org)

<https://doi.org/10.1146/annurev-fluid-122316-045125>

Copyright © 2018 by Annual Reviews.  
All rights reserved

## Keywords

acoustics, flow control, instability, nonlinear dynamical systems, reacting flows, turbulent flows

## Abstract

Nine decades of rocket engine and gas turbine development have shown that thermoacoustic oscillations are difficult to predict but can usually be eliminated with relatively small ad hoc design changes. These changes can, however, be ruinously expensive to devise. This review explains why linear and nonlinear thermoacoustic behavior is so sensitive to parameters such as operating point, fuel composition, and injector geometry. It shows how non-periodic behavior arises in experiments and simulations and discusses how fluctuations in thermoacoustic systems with turbulent reacting flow, which are usually filtered or averaged out as noise, can reveal useful information. Finally, it proposes tools to exploit this sensitivity in the future: adjoint-based sensitivity analysis to optimize passive control designs and complex systems theory to warn of impending thermoacoustic oscillations and to identify the most sensitive elements of a thermoacoustic system.



### ANNUAL REVIEWS **Further**

Click [here](#) to view this article's online features:

- Download figures as PPT slides
- Navigate linked references
- Download citations
- Explore related articles
- Search keywords

## 1. HISTORY AND MOTIVATION

The first scientific reports of thermoacoustic oscillations appeared over two centuries ago (Higgins 1802) and described a phenomenon that was already well known to glass blowers (Sondhaus 1850). The physical mechanism was deduced over one century ago (Rayleigh 1878) and has been used in analysis since at least the 1940s (Crocco & Cheng 1956). The practical consequences of thermoacoustic oscillations have been evident since liquid rocket engine development in the 1930s: They cause thrust oscillations, structural damage, increased heat transfer, and component or payload failure. Despite decades of research by Germany from the 1930s on, by the United States and the USSR during the Cold War (Oefelein & Yang 1993, Culick 2006, Dranovsky 2007), and recently by the gas turbine industry (Lieuwen & Yang 2005), these oscillations remain a severe problem today (Poinsot 2017).

The mechanism that drives thermoacoustic oscillation is similar to that which drives a piston engine. In an idealized piston engine, work is first done on a gas as it is compressed isentropically. The gas then combusts at fixed volume, releasing heat and raising its pressure further. Next, this gas does work as it expands isentropically to its original volume. More work is done by the gas during the expansion phase than is done on it during the compression phase, leading to a net conversion of heat to work. In thermoacoustics, an acoustic wave replaces the piston and a continuous flame replaces the periodically ignited gas. The acoustic wave independently (*a*) perturbs this flame and (*b*) compresses and expands the gas around the flame. If the perturbed flame releases more heat than average during instants of higher local pressure, then more work is done by the gas during the acoustic expansion phase than is done on it during the acoustic compression phase. If this work is not dissipated, then the oscillation amplitude grows and the system is thermoacoustically unstable. Chu (1965) provided a detailed description and analysis of the thermoacoustic mechanism.

There is little alternative to the devices afflicted by thermoacoustic oscillations: Rockets and jet engines have unrivaled power-to-weight ratios, and, in addition, ground-based gas turbines emit less CO<sub>2</sub> per unit of power than coal-fired power stations. In order to achieve high power-to-weight ratios and high efficiencies, these engines all have low acoustic damping and high energy densities: up to 50 GW/m<sup>3</sup> for liquid rockets, 1 GW/m<sup>3</sup> for solid rockets, and 0.1 GW/m<sup>3</sup> for jet engines and afterburners (Culick 2006). Consequently, large amplitude oscillations can be sustained even if the thermoacoustic mechanism is only slightly (approximately 0.1%) efficient for at least one acoustic mode (Huang & Yang 2009).

Development of these engines consists of component tests, sector tests, full combustor tests, and full engine tests. Thermoacoustic instability tends to recur during the later stages and is rarely predicted reliably by component tests and analysis (Lieuwen & McManus 2003, Mongia et al. 2003, Huang & Yang 2009). There are three main reasons for this. First, the efficiency of the thermoacoustic mechanism depends strongly on the time lag between heat release rate and pressure oscillations (Sections 2.3 and 2.4). Second, this time lag depends on hydrodynamic, acoustic, and combustion mechanisms, which scale differently with geometry and pressure and are sensitive to parameters (Section 2.5). Third, this time lag can vary from cycle to cycle, leading to elaborate nonlinear behavior (Section 3). On the positive side, this sensitivity presents opportunities for passive control (Section 2.6) or diagnosis and avoidance of oscillations by analyzing acoustic fluctuations either stochastically (Section 4.1) or with tools from dynamical systems and complex systems theories (Section 4.2).

Important areas that are not covered in this review are (*a*) feedback control (Candel 1992, 2002; McManus et al. 1993; Dowling & Morgans 2005), (*b*) the dynamics of swirling flames (Candel et al. 2014), (*c*) the interaction between hydrodynamic and thermoacoustic instabilities (McManus et al. 1993, Lieuwen 2012, Oberleithner et al. 2015), (*d*) annular combustors and transverse modes

(Worth & Dawson 2013, Bourgoïn et al. 2015, O'Connor et al. 2015, Bauerheim et al. 2016), and (e) computational fluid dynamics (CFD) (Poinsot 2017).

## 2. SENSITIVITY ARISING FROM LINEAR BEHAVIOR

Rocket and gas turbine combustion chambers are designed to operate in intense turbulent flow, without unsteady acoustic oscillations. It is therefore appropriate to perform a linear analysis of acoustic perturbations to the time-averaged turbulent flow. This is known as the triple decomposition and is described by Reynolds & Hussain (1972) for hydrodynamics and by Huang & Yang (2009, section 5.1) for thermoacoustics. Alternatively, a simpler analysis can be performed around a uniform flow, neglecting turbulence (Rayleigh 1896, chapter XXI).

### 2.1. The $n - \tau$ Model for Heat Release

The  $n - \tau$  model was first used by Summerfield (1951) after a 1941 discussion with von Kármán. An acoustic perturbation at a fuel injector causes a downstream heat release rate perturbation some time later (Harrje & Reardon 1972). To leading order (Lieuwen 2012, chapter 12), this can be modeled with a compact flame  $n - \tau$  model, in which the heat release rate fluctuation at position  $\mathbf{x}_f$  and time  $t$  is  $q(\mathbf{x}_f, t) = nu(\mathbf{x}_m, t - \tau)$ , where  $u(\mathbf{x}_m, t - \tau)$  is the acoustic velocity at position  $\mathbf{x}_m$ , time  $\tau$  before time  $t$ , and  $n$  is a constant known as the interaction index. Higher-order terms capture spatial variations in phase, which can be modeled heuristically by setting  $n$  and  $\tau$  to be functions of space (Nicoud et al. 2007). Also,  $u$  can be replaced by the acoustic pressure or the equivalence ratio perturbations, and  $\tau$  can depend on the flow variables (Crocco & Cheng 1956). This model encapsulates the physics required to explain thermoacoustic oscillations, although it misses some details, such as flame cancellation in flames perturbed by the equivalence ratio (Lieuwen 2012). Crocco viewed this model as a “heuristic attempt to analyse combustion instability until superior knowledge of unsteady combustion processes was developed” (Sirignano 2016, p. 175). Although these fundamental processes have since been discovered, usually through detailed experiments (Poinsot et al. 1987), the  $n - \tau$  model is still widely used and, in this review, demonstrates why thermoacoustic oscillations are so sensitive to small changes in  $\tau$ .

### 2.2. A Model Problem

For illustration, we consider oscillations in an open-ended tube from  $x = 0$  to  $X$ , containing gas at uniform density  $\bar{\rho}$ , uniform pressure  $\bar{p}$ , uniform ratio of specific heats  $\gamma$ , and zero mean velocity  $\bar{u}$ . We consider planar acoustic perturbations to the velocity,  $u$ , and pressure,  $p$ . These assumptions prevent entropy and vorticity waves from propagating, allowing an acoustic wave equation to be derived (Nicoud & Wicczorek 2009). A heat source is placed at  $x = x_f$ , with heat release rate  $q(t) = nu(x_m, t - \tau)$  watts per squared meter, where  $n$  is a real constant with units of energy per cubic meter,  $\tau$  is a time delay, and  $x_m$  is the position at which  $u$  is measured (Section 2.1). We neglect viscous and thermal dissipation and the mean density drop across the heat source. The dimensional acoustic momentum and energy equations are

$$\bar{\rho} \frac{\partial u}{\partial t} + \frac{\partial p}{\partial x} = 0, \quad \frac{\partial p}{\partial t} + \gamma \bar{p} \frac{\partial u}{\partial x} = (\gamma - 1)q \delta_D(x - x_f), \quad 1.$$

where  $\delta_D$  is the Dirac delta. These are nondimensionalized with length  $X$ , sound speed  $\bar{c} \equiv \sqrt{\gamma \bar{p} / \bar{\rho}}$ , and pressure  $\bar{p}$  (see **Supplemental Tutorial 1**, section 2). We define  $\gamma' \equiv (\gamma - 1)/\gamma$ .

Three methods are often used to solve Equation 1: the traveling wave framework (Rayleigh 1896, section 245), the Galerkin framework (Zinn & Lores 1971), and the Helmholtz framework

 Supplemental Material

(Nicoud et al. 2007). In all three methods (see **Supplemental Tutorial 1**, section 3), the dimensionless governing equations are expressed as a nonlinear matrix eigenvalue problem,

$$\mathbf{L}(s)\mathbf{q} = 0, \quad 2.$$

where  $\mathbf{q}$  is a state vector that depends on the method, and the matrix  $\mathbf{L}$  depends nonlinearly on the Laplace variable,  $s \equiv s_r + is_i$ , where  $s_r$  is the growth rate and  $s_i$  the frequency. Equivalently,  $\mathbf{L}$  in Equation 2 can be expressed as a function of the Fourier variable,  $\omega \equiv is$ .

In the traveling wave method, downstream-traveling ( $F$ ) and upstream-traveling ( $G$ ) waves are considered upstream ( $F_u, G_u$ ) and downstream ( $F_d, G_d$ ) of  $x_f$ , respectively. With reflection coefficients  $R$  at each end and jump conditions for  $u$  and  $p$  at  $x_f$ , these waves must satisfy

$$\mathbf{L}(s)\mathbf{q} \equiv \begin{bmatrix} (1 + Re^{-s\tau_u}) & -(1 + Re^{-s\tau_d}) \\ (1 - Re^{-s\tau_u}) + (\gamma'ne^{-s\tau})f & (1 - Re^{-s\tau_d}) \end{bmatrix} \begin{bmatrix} G_u \\ F_d \end{bmatrix} = 0, \quad 3.$$

where  $\tau_u \equiv 2x_f/\bar{c}$ ,  $\tau_d \equiv 2(1 - x_f)/\bar{c}$ ,  $f \equiv (e^{-s\tau_{mf}} - Re^{+s\tau_{mf}}e^{-s\tau_u})$ , and  $\tau_{mf} \equiv (x_f - x_m)/\bar{c}$ .

In the Helmholtz method,  $\mathbf{q}$  contains the values of  $p(x_i)$  at grid points  $x = x_i$ . In the Galerkin method,  $u$  and  $p$  are usually projected onto a basis set of  $N$  acoustic modes satisfying the boundary conditions, and  $\mathbf{q}$  then contains their amplitudes. Both become

$$\mathbf{L}(s)\mathbf{q} \equiv (s^2\mathbf{I} + (\gamma'ne^{-s\tau})\mathbf{F} - \mathbf{D}^2)\mathbf{q} = 0, \quad 4.$$

where  $\mathbf{D}^2$  performs  $d^2/dx^2$  and  $\mathbf{F}$  contains information about the measurement point  $x_m$  and flame position  $x_f$ . In the Galerkin framework, the matrix  $\mathbf{D}^2$  is given by  $D_{jk}^2 \equiv -(k\pi)^2\delta_{jk}$ , and, if  $p = 0$  at both ends, then  $F_{jk} \equiv 2k\pi f_{jk}$ , where  $f_{jk} \equiv \cos(j\pi x_m)\sin(k\pi x_f)$ .

### 2.3. Sensitivity Due to Changes in the Relative Phases of $q$ and $p$

One source of sensitivity in thermoacoustics is well known: If  $\tau$  is not small relative to the oscillation period  $T$  of a given acoustic mode, then relatively small changes in  $\tau$  cause large changes in the efficiency of the thermoacoustic mechanism. This was demonstrated theoretically by Crocco & Cheng (1956, section 3.02), described by McManus et al. (1993, section 2.1.6), and shown experimentally by, for example, Noiray et al. (2008).

To demonstrate, we consider an open-ended tube ( $R = -1$ ) as  $n \rightarrow 0$ . For the wave method,  $\det(\mathbf{L}) = 0$  in Equation 3 reduces to  $e^{-2s} = 1$ , with solutions  $s = \pm k\pi i$ , where  $k$  is an integer from 0 to  $\infty$ . For the Galerkin method, Equation 4 reduces to  $N$  uncoupled equations  $s^2 = -(k\pi)^2$ , with the same solutions, with  $k$  from 0 to  $N$ . These have period  $T = 2/k$  and are the natural acoustic modes of the system. For the Helmholtz method, the solutions approach these as the number of grid points increases. Using the Galerkin method, we consider how the heat release rate perturbs these modes. When  $n$  is of order  $\epsilon$ , each eigenvalue  $\pm k\pi i + \mathcal{O}(\epsilon)$  of Equation 4 has a corresponding eigenvector whose  $k$ -th element is  $\mathcal{O}(1)$  and other elements are  $\mathcal{O}(\epsilon)$ . The coupling terms are therefore  $\mathcal{O}(\epsilon)^2$  and can be neglected when compared with the self-coupling term, which is  $\mathcal{O}(\epsilon)$ . We can therefore consider each mode in Equation 4 separately such that the matrix-vector product  $\mathbf{L}(s)\mathbf{q}$  becomes a function  $L(s)$  multiplied by the  $k$ -th element of  $\mathbf{q}$ :

$$L(s)\mathbf{q}_k \equiv \left[ s^2 + \epsilon(2k\pi\beta e^{-s\tau}) + (k\pi)^2 \right] \mathbf{q}_k = 0, \quad 5.$$

where  $\beta \equiv \gamma'nf_{kk}$  and  $f_{kk} \equiv \cos(k\pi x_m)\sin(k\pi x_f)$ . Substituting  $s = s_0 + \epsilon s_1$  gives  $s_0 = \pm k\pi i$  at  $\mathcal{O}(1)$  and  $s_1 = i\beta e^{-s_0\tau}$  at  $\mathcal{O}(\epsilon)$ . The growth rate  $s_r$  is therefore  $\beta \sin(k\pi\tau)$ , which reveals some useful physical insights. First, for  $k\tau \ll 1$ , the growth rate is proportional to  $\tau$ , which, for cases in which  $f_{kk} > 0$ , is equivalent to the demonstrations by Candel (2002) and Ducruix et al. (2003)

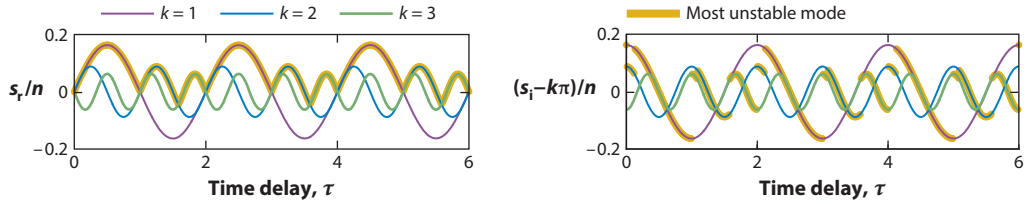


**Figure 1**

Rescaled growth rate  $s_r$  (left) and frequency  $s_i$  (right) as functions of time delay  $\tau$  for the  $k$ -th modes of a Rijke tube with  $p = 0$  at both ends. The most unstable mode (thick yellow line) switches often as  $\tau$  varies. The Laplace variable,  $s$ , is calculated with a 400-mode Galerkin method with  $x_m = 0.20$ ,  $x_f = 0.25$ ,  $n = 1$ , and  $\gamma = 1.4$ . Identical results are obtained using the traveling wave and Helmholtz methods.

that the time lag is destabilizing. Second, the growth rates of each mode oscillate as  $\tau$  varies, and the most unstable mode switches often (**Figure 1**). Third, through  $f_{kk}$ , the growth rate is sensitive to the measurement position  $x_m$  and the flame position  $x_f$  and becomes more so as  $k$  increases.

This model implies that mode switching with  $\tau$  will become endemic for large  $k$ . This is misleading, however, because the model contains no damping or acoustic radiation. In reality, higher-frequency modes are damped by viscosity and geometry, as in a rocket engine's convergent nozzle (Crocco & Cheng 1956), and mode switching is not so severe. Nevertheless, this explains why thermoacoustic oscillation is so prevalent in combustors with high energy densities and many lightly damped longitudinal modes, transverse modes, and combined longitudinal and transverse modes: A geometry must be found at which every mode is thermoacoustically stable across the entire operating range. For the Apollo F1 engine, this required 2,000 full-scale tests (Oefelein & Yang 1993).

## 2.4. Sensitivity Due to Eigenvalue Degeneracy

Another source of sensitivity appears near operating points at which two or more modes have the same frequency and growth rate, i.e., when eigenvalues are degenerate. It is obvious that annular combustors support degenerate eigenvalues, corresponding to pairs of modes that are identical apart from the rotation direction. It is less obvious that longitudinal modes can also be degenerate (Crocco & Cheng 1956, figure 5). We consider the single-mode Galerkin method in Equation 5 with  $\epsilon \sim 1$  to show that this occurs at realistic parameter values:

$$L(s) \equiv s^2 + 2k\pi\beta e^{-s\tau} + (k\pi)^2 = 0. \quad 6.$$

**Figure 3** shows that the coupling with higher modes has no qualitative influence on this result. Changes to  $L$  can be expressed as  $\delta L = \partial L/\partial s|_{\tau,\beta} \delta s + \partial L/\partial \beta|_{s,\tau} \delta \beta + \partial L/\partial \tau|_{s,\beta} \delta \tau$  (for full details of this analysis, see Magri et al. 2016a). Because Equation 6 must remain satisfied as  $\tau$  and  $\beta$  vary,  $\delta L$  equals 0 and the sensitivities of  $s$  to  $\beta$  and  $\tau$  can be written as

$$\left. \frac{\partial s}{\partial \beta} \right|_{L,\tau} = -\frac{\partial L/\partial \beta|_{s,\tau}}{\partial L/\partial s|_{\tau,\beta}}, \quad \left. \frac{\partial s}{\partial \tau} \right|_{L,\beta} = -\frac{\partial L/\partial \tau|_{s,\beta}}{\partial L/\partial s|_{\tau,\beta}}. \quad 7.$$

This breaks down when the eigenvalues are exactly degenerate, which occurs when  $\partial L/\partial s = 0$ . Around these points, where  $|\partial L/\partial s|$  is small, each eigenvalue is extremely sensitive to  $\beta$ ,  $\tau$ , and, indeed, every model parameter. The solutions to  $L = \partial L/\partial s = 0$  all lie on the line  $\beta\tau = \pm e^{-1}$  and satisfy  $s_1\tau = \tan(s_1\tau)$ , where  $s_1\tau = \sqrt{1 - (k\pi\tau)^2}$ . These lines are shown in **Figure 2a**, next to the sensitivities  $\partial s/\partial \tau$  and  $\partial s/\partial \beta$  when  $k = 1$ . As  $k$  increases, points of extreme sensitivity cluster ever more closely on the lines  $\beta\tau = \pm e^{-1}$ . **Table 1** shows that  $\max(\beta\tau)$  exceeds  $e^{-1} = 0.3769$  in many practical systems.

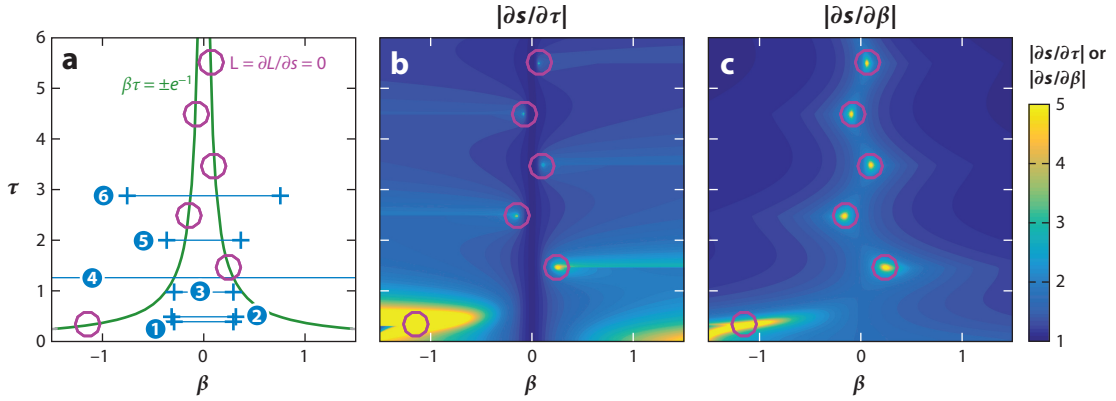


**Figure 2**

(a) Points of eigenvalue degeneracy (purple circles) for the  $k = 1$  mode of Equation 5. As  $k$  increases, these points cluster more closely on the green lines  $\beta\tau = \pm e^{-1}$ . The numbered blue lines show the ranges of  $(\beta, \tau)$  for the practical thermoacoustic systems in **Table 1**. (b,c) Numerically calculated (b)  $|\partial s/\partial \tau|$  and (c)  $|\partial s/\partial \beta|$ , showing that  $s$  is very sensitive to the parameters around the degenerate points.

### 2.5. Sensitivity Due to the Parameters

Sections 2.3 and 2.4 show why the thermoacoustic mechanism's efficiency is so sensitive to  $n$  and  $\tau$ . In turn, these parameters are sensitive to factors such as the operating conditions, injector geometry, and fuel composition. For example, Durox et al. (2009) found that  $\tau$  changes by a factor of 2.8 when, at one operating condition, a flame is anchored differently. Prieur et al. (2016) found that a change to the cup angle of a swirl injector changes  $\tau$  by a factor of 1.5. Ćosić et al. (2014) found that a 3% change in the fuel flow rate of a partially premixed swirl-stabilized gaseous fuel flame caused the gain to change by more than 30% and the phase by up to 20°. Processes often overlap, leading to more than one time delay (Candel 2002, figure 5; Komarek & Polifke 2010, Sirignano 2016, section 4) or a distribution of time delays (Bade et al. 2013). The sensitivity of  $\tau$  is even more extreme in liquid fuel flames because the heat release rate is affected by jet breakup,

**Table 1** Typical values of  $n$  and  $\tau$  for different flames and thermoacoustic systems

Device	Dimensional values						Dimensionless values			
	$\bar{q}^*$ (kW)	$A^*$ (cm <sup>2</sup> )	$\bar{u}^*$ (ms <sup>-1</sup> )	$\bar{p}^*$ (bar)	$\tau^*$ (ms)	$f^*$ (Hz)	$n$	$\tau$	$\max(\beta)$ (= $\gamma'n$ )	$\max(\beta\tau)$ (= $\gamma'n\tau$ )
Hot wire Rijke tube (Rigas et al. 2016)	0.20	20.0	1.0	1.0	1.0	200	1.00	0.40	0.29	0.114
Swirl flame (Kim et al. 2010b)	73.5	93.7	70	1.0	1.0	250	1.12	0.50	0.32	0.16
Liquid fuel swirl flame (Yi & Santavicca 2010)	60	78.5	75	1.0	0.83	600	1.02	1.00	0.29	0.29
Multicone flame (Noiray et al. 2008)	14	38.5	3.43	1.0	0.9	700	10.6	1.26	3.03	2.846
Swirl flame (Kim et al. 2010a)	72.7	93.7	60	1.0	5.0	200	1.29	2.00	0.37	0.74
Swirl flame (Balachandran et al. 2005)	10	38.4	9.9	1.0	4.4	330	2.63	2.90	0.75	2.183

atomization, vaporization, and combustion (Crocco 1951, Summerfield 1951, Zhu et al. 2002, Yi & Santavica 2010). This extreme sensitivity introduces considerable systematic uncertainty into models (Section 2.7).

## 2.6. Exploiting Extreme Sensitivity with Adjoint Methods

When safety and endurance are paramount, thermoacoustic oscillations must be suppressed passively (McManus et al. 1993, Richards et al. 2003, Lieuwen & Yang 2005) by, for example, modifying the time delay (Steele et al. 2000); shielding the fuel injectors with baffles (Oefelein & Yang 1993); adding acoustic dampers (Eldredge & Dowling 2003); or adding quarter-wave tubes, Helmholtz resonators (Zinn 1970, Gysling et al. 2000, Bellucci et al. 2004), or dynamic phase converters (Noiray et al. 2009).

The extreme sensitivity described in Sections 2.3–2.5 explains why thermoacoustic oscillations can be suppressed by relatively small design changes (Oefelein & Yang 1993, Mongia et al. 2003, Dowling & Morgans 2005). These changes tend to be made ad hoc. A more systematic approach is desirable but requires (a) a model that can reliably predict linear thermoacoustic behavior, (b) a cheap way to obtain the sensitivity of the linear growth rate to all parameters of the model, and (c) a combination of this sensitivity information with practical constraints to find the optimal passive control mechanism.

For step *b*, adjoint methods (Luchini & Bottaro 2014) are ideal because only a handful of thermoacoustic modes are unstable, but many parameters can be altered (see section 4 of **Supplemental Tutorial 1**). Adjoint methods were introduced into linear stability analysis independently by Hill (1992, 1995) and Chomaz (1993). They have since been extended to nonmodal stability theory and nonlinear time-dependent flows (Schmid 2007). Using the nonlinear adjoint method, Juniper (2011) found the smallest initial perturbation that causes triggering in a hot wire Rijke tube (see the sidebar titled Bypass Transition to Turbulence and Triggering in Thermoacoustics). Using the linear adjoint method, Magri & Juniper (2013, 2014) devised optimal passive control strategies for thermoacoustic instability in Rijke tubes, and Mensah & Moeck (2017) devised optimal acoustic damper placement in an annular combustor.

The adjoint problem is constructed by premultiplying Equation 2 by another vector  $\mathbf{q}^\dagger$ :

$$\mathbf{q}^{\dagger H} \mathbf{L}(s) \mathbf{q} = 0, \quad 8.$$

where  $^H$  is the conjugate transpose. For a given eigenvalue,  $s$ , the right eigenvector  $\mathbf{q}$  is defined such that Equation 8 is satisfied for arbitrary  $\mathbf{q}^\dagger$ . Similarly, the left eigenvector  $\mathbf{q}^\dagger$  is defined such that Equation 8 is satisfied for arbitrary  $\mathbf{q}$ . Once an eigenmode  $(\mathbf{q}^\dagger, s, \mathbf{q})$  has been found, the

 **Supplemental Material**

### BYPASS TRANSITION TO TURBULENCE AND TRIGGERING IN THERMOACOUSTICS

Bypass transition to turbulence and triggering in thermoacoustics are manifestations of similar nonlinear behavior. Both require a system to be bistable. In hydrodynamics, one stable state is the steady laminar solution and the other is typically a chaotic attractor. In thermoacoustics, one stable state is the steady solution and the other is typically a periodic solution. These chaotic or periodic solutions can be reached from many initial states. Of these states, the one with the smallest initial energy is called the minimal seed. In thermoacoustics, growth from the minimal seed exploits transient growth around the unstable periodic solution (Juniper 2011). In hydrodynamics, the mechanism seems to be similar, although with many more unstable periodic solutions (Kerswell 2018).

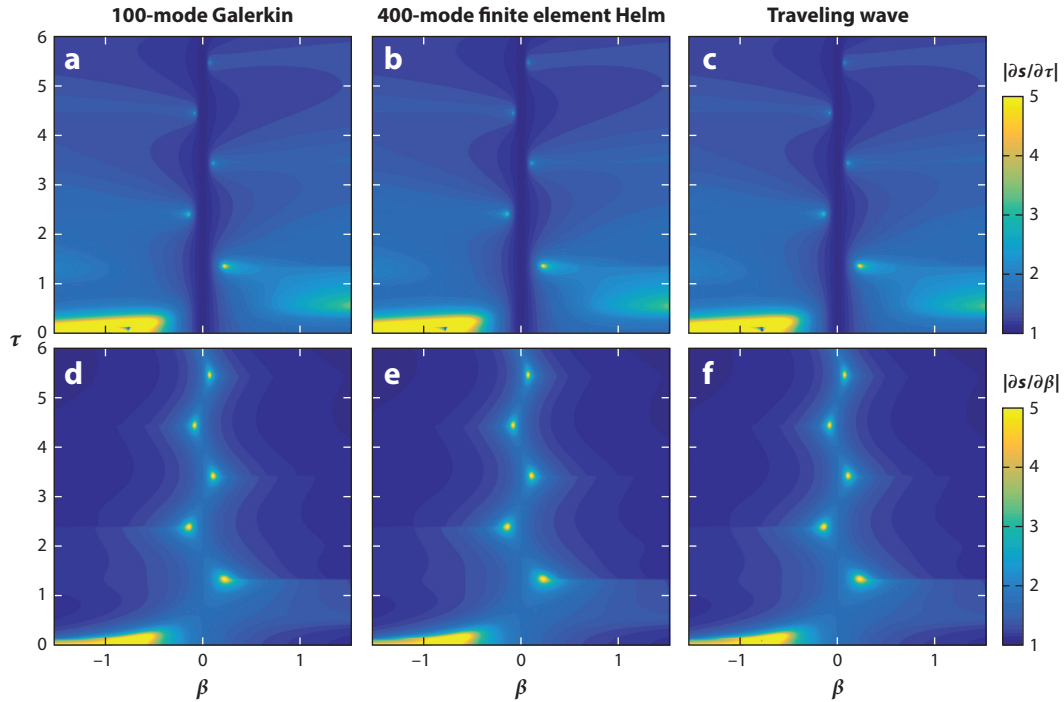


**Figure 3**

The sensitivities  $|\partial s/\partial \tau|$  (a–c) and  $|\partial s/\partial \beta|$  (d–f) calculated with the adjoint method in Equation 9 for (a,d) the 100-mode Galerkin method, (b,e) the 400-mode finite element Helmholtz method, and (c,f) the wave method. The results calculated with each method are identical and are also close to those for the single-mode Galerkin model in **Figure 2**, which has the same parameter values:  $x_m = 0.20$ ,  $x_f = 0.25$ , and  $\gamma = 1.4$ .

sensitivity of  $s$  to every parameter  $[\cdot]$  is found cheaply (Magri et al. 2016a) with

$$\frac{\partial s}{\partial [\cdot]} = -\frac{\mathbf{q}^{\dagger H} (\partial \mathbf{L} / \partial [\cdot]) \mathbf{q}}{\mathbf{q}^{\dagger H} (\partial \mathbf{L} / \partial s) \mathbf{q}}, \quad \text{which becomes} \quad \frac{\partial s}{\partial [\cdot]} = \frac{\mathbf{q}^{\dagger H} (\partial \mathbf{L} / \partial [\cdot]) \mathbf{q}}{\mathbf{q}^{\dagger H} \mathbf{B} \mathbf{q}} \quad \text{if} \quad \mathbf{L} = \mathbf{A} - \mathbf{B}s. \quad 9.$$

**Figure 3** shows the parameter sensitivities of **Figure 2**, recalculated using adjoint methods for a 100-mode Galerkin method, a 400-element Helmholtz method, and the wave method. This confirms that the points of extreme sensitivity, which were found analytically for the single-mode Galerkin model, exist around the same parameter values for the more accurate models. We can then multiply  $\partial s/\partial n$  and  $\partial s/\partial \tau$  by the sensitivity of  $n$  and  $\tau$  to the injection conditions, derived from a separate adjoint calculation. An approach similar to that of Tammisola & Juniper (2016) would give the influence of the injector geometry on the heat release rate,  $n(\mathbf{x})$ , and time delay,  $\tau(\mathbf{x})$ , fields and, thus, the eigenvalue.

Adjoint methods also provide base state sensitivities, which can be used for physical insight or in gradient-based optimization algorithms. For example, **Figure 4a,b** shows the pressure and velocity of the first eigenmode of Equation 1, calculated with a Helmholtz method in which the measurement function,  $w$ , the interaction index,  $n$ , and the time delay,  $\tau$ , are functions of  $x$ . **Figure 4e–g** shows the sensitivity of  $s$  to local increases in  $w(x)$ ,  $n(x)$ , and  $\tau(x)$ , respectively. These show that  $\partial s/\partial w(x)$  approximately follows  $u(x)$ , which is because  $q \propto \int wu \, dx$ ; that  $\partial s/\partial n(x)$  approximately follows  $p(x)$ , which is because the influence of  $q$  on the growth rate is proportional to  $\int np \, dx$ ; and that  $\tau$  is only influential in the reaction zone.

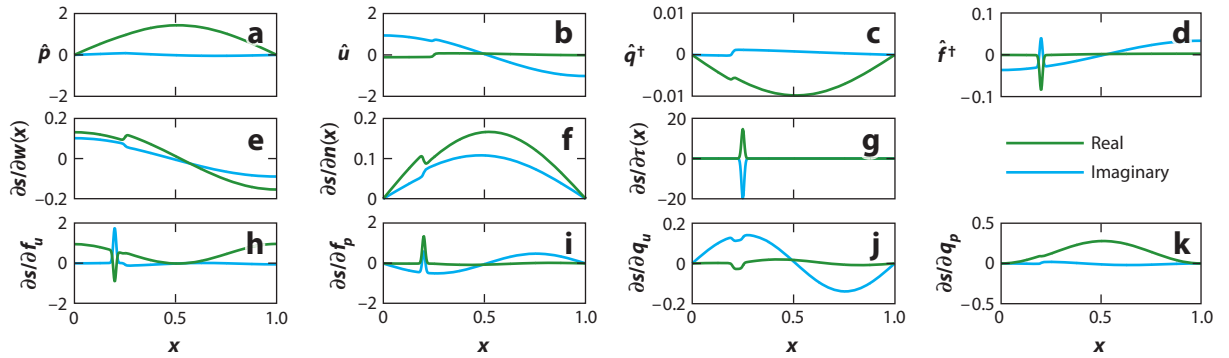


**Figure 4**

(a) Pressure  $\hat{p}$  and (b) velocity  $\hat{u}$  eigenfunctions for the finite element Helmholtz method with  $x_m = 0.20$ ,  $x_f = 0.25$ ,  $n = 1$ ,  $\tau = 0.3416$ , and  $\gamma = 1.4$ . (c,d) Receptivities to external forcing of (c) the energy or mass equation  $\hat{q}^\dagger$  and (d) the momentum equation  $\hat{f}^\dagger$ . (e–k) The sensitivity of the growth rate  $s_r$  (green) and frequency  $s_i$  (blue) to local changes in the (e) measurement function  $w(x)$ ; (f) interaction index  $n(x)$ ; (g) time delay  $\tau(x)$ ; (h) feedback  $\partial s/\partial f_u$  from velocity into the momentum equation; (i) feedback  $\partial s/\partial f_p$  from pressure into the momentum equation; (j) feedback  $\partial s/\partial q_u$  from velocity into the energy or mass equation; and (k) feedback  $\partial s/\partial q_p$  from pressure into the energy or mass equation.

Adjoint methods also provide receptivity fields, which show where external forcing most influences the eigenvalue or oscillation amplitude (Chomaz 2005, equation 9). **Figure 4c** shows the receptivity,  $q^\dagger$ , of the energy or mass equation to an oscillating heat or mass input, whereas **Figure 4d** shows the receptivity,  $f^\dagger$ , of the momentum equation to an oscillating force.

Adjoint methods also provide feedback sensitivities. Any linear feedback mechanism can be expressed as a sum of six basic feedback mechanisms: from each of the two direct variables (pressure and velocity) into each of the three governing equations (mass, momentum, and energy). For Equation 1, this reduces to four mechanisms because the mass and energy equations are equivalent. **Figure 4b–k** shows how each basic feedback mechanism affects  $s$ . The influence of any feedback device can be calculated from these. For example, a mesh with drag coefficient  $C_D$  causes a linearized local force  $f = -C_D \rho U u \equiv f_u u$ , where  $U$  is the mean velocity. The sensitivity  $\partial s/\partial C_D$  is  $(df_u/dC_D)(\partial s/\partial f_u) = -\rho U (\partial s/\partial f_u)$ , the negative of the real growth rate in **Figure 4b**. This shows that the mesh damps oscillations most effectively when placed at the ends of the tube, which has been confirmed experimentally by Rigas et al. (2016). Another example is a Helmholtz resonator, which is driven by the pressure field and forces the mass equation. Its influence on  $s$  is proportional to  $\partial s/\partial q_p$ , which is proportional to  $\hat{p}q^\dagger$ . If the system were self-adjoint, this would equal  $\hat{p}^2$ , which is often used to guide the placement of Helmholtz resonators. All thermoacoustic systems are non-self-adjoint (Balasubramanian & Sujith 2008), however, so  $\hat{p}q^\dagger$  is a more accurate guide than  $\hat{p}^2$ .

## 2.7. Uncertainty Due to Extreme Sensitivity

The systematic approach in Section 2.6 requires an accurate thermoacoustic model. The prevailing approach is to deduce  $n$  and  $\tau$  (or, equivalently, a flame transfer function; see the sidebar titled The Flame Transfer Function) from experiments or CFD. This can be extended to a flame transfer matrix (Paschereit et al. 2002), which is equivalent to an  $n - \tau$  model that depends on pressure as well as velocity (Truffin & Poinot 2005). However, extreme sensitivity to parameters (Sections 2.3–2.5) can introduce considerable systematic error. To reduce this error, experiments must be performed on a faithful copy of the engine at realistic operating conditions, and CFD has to capture

## THE FLAME TRANSFER FUNCTION

The flame transfer function (FTF) is defined as  $F(\omega) \equiv (q'(\omega)/\bar{q})/(u'(\omega)/\bar{u})$ , where  $q$  is the heat release rate,  $u$  is the velocity at a measurement point,  $\omega$  is the angular frequency,  $\bar{\cdot}$  denotes the mean, and  $\cdot'$  denotes fluctuation ( $u$  can be replaced by  $p$  if this is more appropriate). The FTF can be expressed in terms of the impulse response,  $g(t)$ , and, thus, as a sum of  $n - \tau$  models via  $F(\omega) = \int_0^\infty g(t) \exp(-i\omega t) dt \approx \sum_{m=1}^M n_m e^{-i\omega \tau_m}$ , where  $n_m \equiv \Delta \tau g(\tau_m)$  and  $\tau_m \equiv m \Delta \tau$  (Macquisten et al. 2014).

all feedback mechanisms. This can work for gaseous flames (Bade et al. 2013) but is difficult to generalize, particularly to liquid fuels. A possible solution is to combine adjoint sensitivity analysis (Section 2.6) with uncertainty quantification (Magri et al. 2016b) and calibrate model parameters using automated experiments (Rigas et al. 2016) and inverse uncertainty quantification. Parameters learned on highly instrumented and automated laboratory rigs can then become priors for, and be updated on, increasingly realistic rigs.

### 3. SENSITIVITY ARISING FROM NONLINEAR BEHAVIOR IN THE ABSENCE OF NOISE

There are three main types of nonlinearity in thermoacoustics. The first is gas dynamic nonlinearity (Rankine 1870), which is mainly relevant to rocket motors. The second is damping nonlinearity due to acoustic radiation (Heckl 1990; Matveev 2003a,b), attenuation by suspended particles (Culick 1971), and baffles and orifices (Crocco 1969). The third, and most important, is flame nonlinearity, which can be measured experimentally (Noiray et al. 2008), modeled (Dowling 1997), or simulated with CFD (Poinsot 2017). We introduce a generic nonlinear saturation or driving term in Section 3.1 and the flame describing function (FDF) in Section 3.2. In Section 3.3, we relax the assumption that the acoustics are harmonic and show that the resultant periodic solutions can be unstable to nonperiodic behavior. In Section 3.4, we relax the assumption that the solutions are periodic, which reveals the prevalence of elaborate nonlinear behavior such as quasiperiodicity and chaos, as seen in experiments.

#### 3.1. Sensitivity Due to Subcritical Bifurcations and Bistability

After the Apollo program, Crocco (1969) wrote with misplaced optimism that “rockets can now be made linearly stable without too much difficulty” and asked, “is it possible, in the case of linear stability, that disturbances above a certain amplitude may become amplified?” (p. 86). He called this “nonlinear or triggered instability” (p. 86). By 1969, there had been many experimental and theoretical studies into triggering (Culick 2006, section 7; Sirignano 2016, section 5), and it has since been observed in gas turbines (Lieuwen 2002, Lieuwen & Banaszuk 2005). The field of nonlinear dynamical systems (Strogatz 1994) provides a robust framework to explain triggering and the sensitivity that it causes. In this framework, stability is a purely linear concept, referring to the behavior of infinitesimal perturbations to a solution of the governing equations. This solution can be steady or periodic in time, and it is stable (unstable) if the perturbations decay (grow) in time. A nonlinear instability is therefore more rigorously described as a stable periodic solution, and triggering is the transition from the basin of attraction of a steady solution to the basin of attraction of a periodic solution (see **Supplemental Tutorial 2**, section 2).

To demonstrate, we add a small linear damping or driving term  $\epsilon\zeta\dot{u}_k$  and a small nonlinear saturation or driving term  $\epsilon\xi u_k^2\dot{u}_k$  to Equation 6 in the time domain:

$$\ddot{u}_k + \epsilon(\xi u_k^2 - \zeta)\dot{u}_k + (k\pi)^2 u_k = -2k\pi\beta u_k(t - \tau). \quad 10.$$

Regarding sensitivity, there are two important but unsurprising features (Suchorsky et al. 2010). First, the point at which the steady solution becomes unstable to an oscillation (the Hopf bifurcation) is particularly sensitive to  $\tau$ , as expected from the linear analysis in Section 2. Second, around this point, the saturated amplitude is highly sensitive to all parameters. Further, if  $\xi < 0$ , then the Hopf bifurcation is subcritical and connects to an unstable periodic solution, which can be observed experimentally (Jegadeesan & Sujith 2013). This is usually followed by a fold bifurcation to a stable periodic solution. Subcritical bifurcations are dangerous because systems can trigger abruptly from the steady solution to the stable periodic solution and be unable to return until parameters are reduced beyond those at the fold bifurcation. If the system is highly non-normal, transient growth of background noise can cause triggering (see the sidebar titled *Bypass Transition to Turbulence and Triggering in Thermoacoustics*).

From the point of view of sensitivity, it is useful to determine whether a Hopf bifurcation is supercritical or subcritical. If the system cannot be reduced to a single equation, such as Equation 10, a weakly nonlinear analysis can be used instead, based on an asymptotic expansion of the governing equations near the Hopf bifurcation (Landau 1944). This has been used widely in studies of hydrodynamic stability (Chomaz 2005), e.g., for vortex shedding behind a cylinder (Sipp & Lebedev 2007), and compares well with experimental results (Provansal et al. 1987). This has also been used in studies of thermoacoustic stability (Juniper 2012, Subramanian et al. 2013, Orchini et al. 2016). Supercritical and subcritical Hopf bifurcation are observed both in weakly nonlinear analysis and in experiments (Moeck et al. 2008, Kabiraj et al. 2012b).

### 3.2. Analysis with the Flame Describing Function

A weakly nonlinear analysis (Section 3.1) cannot describe the fully nonlinear behavior. One practical approach is the describing function (Gelb & Vander Velde 1968), in which the flame response is measured as a function of the forcing frequency and amplitude. The acoustic equations are solved in the frequency domain at different amplitudes (Dowling 1997). Limit cycles exist at combinations of amplitudes and frequencies at which the growth rate is zero, and their stability can be assessed. Once a flame's behavior has been measured, the behavior of any thermoacoustic network containing that flame can be inferred provided that the flame is not changed significantly by the new environment. This was exploited particularly thoroughly by Noiray et al. (2008), who compared experimental results with theoretical predictions for a thermoacoustic system containing a matrix of multiple conical premixed flames. The method has also been applied to a ducted flame with a simple saturation model (Dowling 1997), a flame behind a flame holder (Dowling 1999), a single conical premixed flame (Karimi et al. 2009, Hemchandra 2012), a round bluff-body stabilized nonswirling turbulent flame (Balachandran et al. 2005, Armitage et al. 2006, Han et al. 2015), and turbulent premixed or partially premixed swirling flames (Bellows et al. 2007, Shreekrishna et al. 2010, Palies et al. 2011, Schimek et al. 2011, Krediet et al. 2012, Ćosić et al. 2014).

The FDF is obtained by forcing harmonically over a range of frequencies and amplitudes. Because the acoustic field is harmonic, the work done by any heat release rate oscillations at higher harmonics integrates to zero over a cycle. Therefore, the FDF needs to consider only the heat release rate at the forcing frequency. This simplifies the analysis but embeds a questionable assumption: that the acoustics are harmonic in time.

### 3.3. Analysis with Continuation Methods

If the acoustics and heat source models are coupled into a nonlinear dynamical system, then periodic solutions, harmonic or not, can be found with continuation methods. These methods have been applied to thermoacoustics with nonlinear gas dynamics (Jahnke & Culick 1994), nonlinear heat release rate (Ananthkrishnan et al. 2005), and nonlinear time-delayed heat release rate (Subramanian et al. 2010, Juniper 2011). The above models contain around  $10^1$  degrees of freedom (DOF). Simulation of the flame requires at least  $10^2$  to  $10^3$  DOF, however, and matrix-free continuation methods (Waugh et al. 2013, 2014) must be used.

Figure 5a shows periodic solutions for a ducted conical premixed flame as a function of the flame aspect ratio and flame position. The stability of these solutions is determined by the Floquet

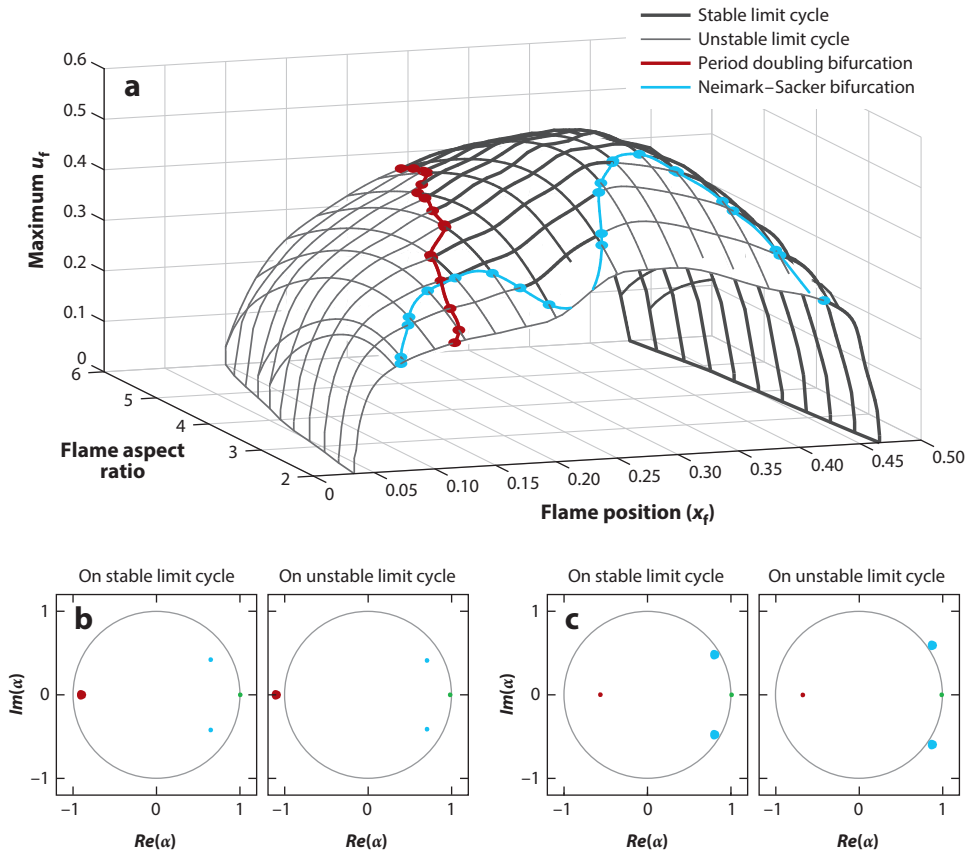
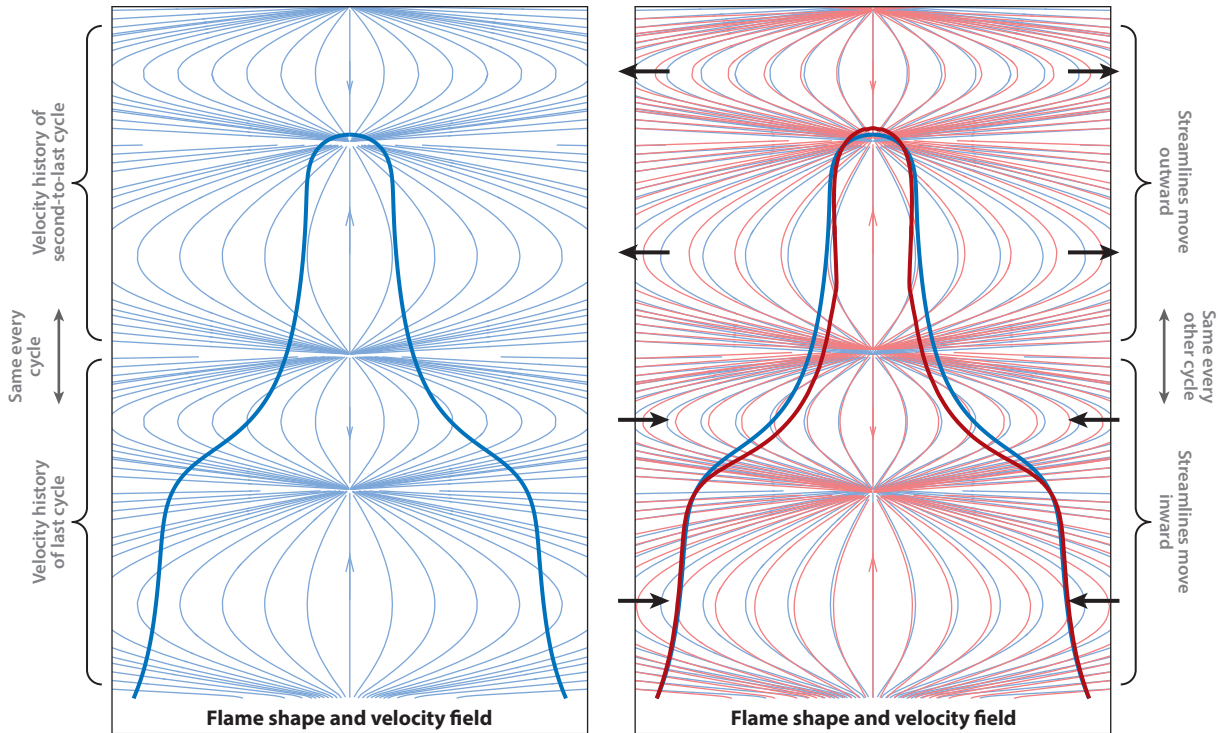


Figure 5

(a) Maximum acoustic velocity at the flame,  $u_f$ , for periodic thermoacoustic oscillations of a conical premixed Bunsen flame in a duct. These oscillations are found with a continuation method as a function of the flame aspect ratio and the flame position in the duct. The stability of these oscillations is determined by examining the Floquet multipliers,  $\alpha$ . The green dots indicate the marginally stable Floquet multiplier corresponding to a perturbation in the direction of the limit cycle. (b) For a period doubling bifurcation, a Floquet multiplier (red dot) crosses the unit circle at  $\alpha = -1$ . (c) For a Neimark-Sacker bifurcation to quasiperiodic behavior, a pair of Floquet multipliers (cyan dots) crosses the unit circle at  $Im(\alpha) \neq 0$ . This continuation analysis reveals that periodic solutions are often unstable. Figure adapted with permission from Waugh et al. (2014, figures 5b, 13, and 15).



**Figure 6**

(a) The flame shape (*dark blue lines*) and streamlines of the acoustic velocity field (*light blue lines*) at one moment of the periodic solution at the onset of the period doubling bifurcation in **Figure 5**. (b) The red lines indicate the flame shape and streamlines in panel *a* when perturbed in the direction of the Floquet mode that causes the period doubling bifurcation. The blue lines indicate the unperturbed lines from panel *a*. Figure adapted with permission from Waugh et al. (2014, figure 17).

multipliers,  $\alpha$ , of small perturbations to the solutions (**Figure 5b,c**). If  $|\alpha| > 1$ , then the periodic solution is unstable (Schmid & Henningson 2001, section 6.4.1). Further, if  $\alpha$  is a positive real number greater than 1, then the growing perturbation has the same period as the original solution (this is the only situation that can be analyzed with the FDF). If  $\alpha$  is a negative real number less than  $-1$ , then the corresponding perturbation swaps direction each cycle, thereby growing with double the period of the original solution (**Figure 5b**). If the argument of  $\alpha$  is  $\pi/k$ , where  $k$  is an integer, then the perturbation grows with  $k$  times the period of the original periodic solution. If the argument is  $\pi/k$ , where  $k$  is not an integer, then a quasiperiodic solution grows. This is known as a Neimark–Sacker bifurcation (**Figure 5c**).

The eigenfunctions of the Floquet multipliers reveal the physical behavior at each bifurcation. **Figure 6a** shows a snapshot of a finite amplitude periodic solution, in which the flame contains two wrinkles, seen most clearly in the streamlines. At the period doubling bifurcation, this motion becomes unstable to a perturbation containing a single wrinkle along the length of the flame (**Figure 6b**). This grows toward a period 2 limit cycle (Section 3.4). (The motion is not equivalent to the superposition of two infinitesimal primary instabilities of the corresponding steady flow.) This connection between wrinkle propagation and dynamical states has been shown experimentally by Vishnu et al. (2015).

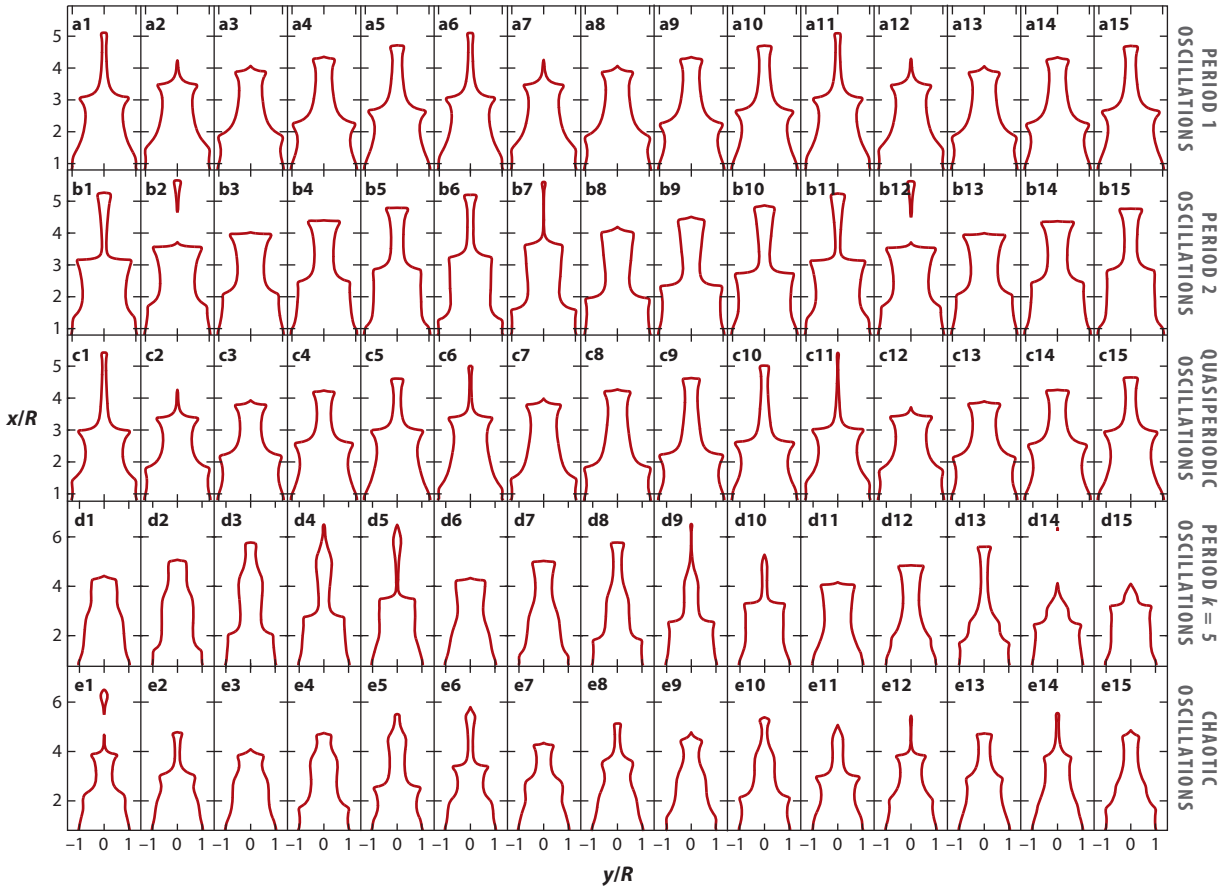


**Figure 7**

Numerical simulations showing instantaneous flame surfaces for different types of self-excited oscillations of a two-dimensional slot-stabilized premixed flame in a duct. The images depict (a) period 1 oscillations, repeated every 5 frames; (b) period 2 oscillations, repeated every 10 frames; (c) quasiperiodic oscillations; (d) period  $k = 5$  oscillations; and (e) chaotic oscillations. Adapted from Kashinath et al. (2014, figure 7).

### 3.4. Sensitivity Due to Elaborate Nonlinear Flame Dynamics

The assumption of periodicity must be dropped for the instabilities in Section 3.3 to develop. Although the thermoacoustic mechanism (Rayleigh 1878) does not require periodicity, most analyses require oscillations to be periodic at zeroth order, with a slowly varying amplitude at first order. Examples include energy analysis (Chu 1965), two-timing (Strogatz 1994), and the method of averaging (Culick 2006). In reality, the phase difference between pressure and heat release can vary rapidly, altering the net conversion from heat to work each period. This causes the oscillations to be more elaborate than the periodic assumption allows.

For example, the period doubling bifurcation in **Figure 6** leads to a period 2 limit cycle, shown for a similar flame in **Figure 7b** (frames 1–15). Pinch off and burnout occur at different moments in the first (frames 1–5) and second periods (frames 6–10). This alternating phase difference between the heat release rate and pressure converts alternating amounts of heat into work each period, causing the time series and twin loop phase portrait in **Figures 8b** and **9b**.

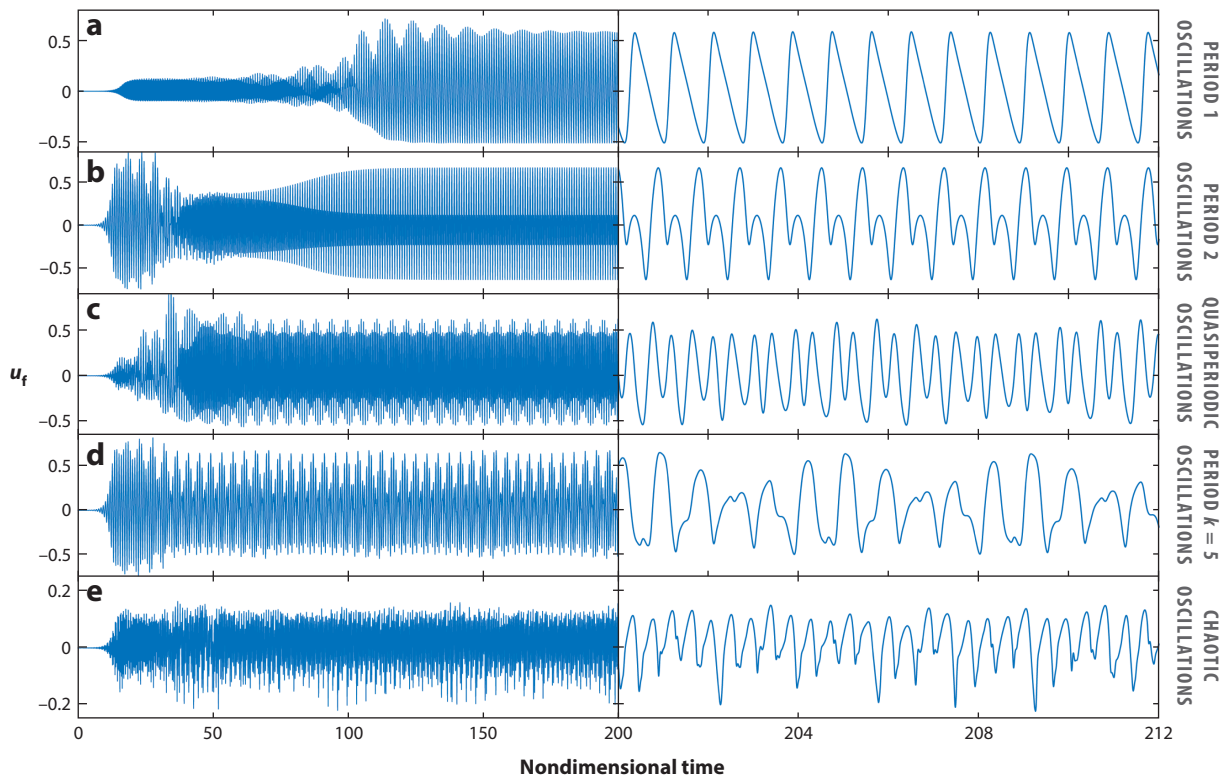


**Figure 8**

Numerical simulations showing the acoustic velocity at the flame,  $u_f$ , for different types of self-excited oscillations of a two-dimensional slot-stabilized premixed flame in a duct. The images depict (a) period 1 oscillations, (b) period 2 oscillations, (c) quasiperiodic oscillations, (d) period  $k = 5$  oscillations, and (e) chaotic oscillations. Adapted from Kashinath et al. (2014, figure 8).

Similarly, the Neimark–Sacker bifurcation (**Figure 5c**) leads to quasiperiodicity, shown for a similar flame in **Figure 7c** (frames 1–15). The phase difference between pressure and heat release rate advances each period by a noninteger portion of the period, causing a toroidal phase portrait (**Figures 8c** and **9c**). If the phase difference advances instead by a fraction ( $1/k$ ) of the period, then period  $k$  oscillations occur (**Figures 8d** and **9d**). It can also advance chaotically (**Figures 8e** and **9e**). This behavior is mapped as a function of the flame position,  $x_f$ , in **Figure 10a**. It is rarely periodic and switches abruptly with  $x_f$ .

Periodic, quasiperiodic, frequency-locked, and chaotic behaviors have been observed in a gas turbine (Gotoda et al. 2011), as well as in combustors containing a backward-facing step (Sterling & Zukoski 1991), a ducted V-flame (Vishnu et al. 2015), premixed flames (Kabiraj et al. 2012b), and multiple flames (Kabiraj & Sujith 2012, Kabiraj et al. 2012a). **Figure 10b** shows a bifurcation diagram (Kabiraj et al. 2012a), and **Figure 11** shows phase portraits of the experiments by (Kabiraj et al. 2012b).

#### 4. COMPLEX DYNAMICS OF THERMOACOUSTIC SYSTEMS WITH TURBULENT FLOW

Traditionally, an experimental or CFD measurement is assumed to consist of a signal plus noise. The signal is extracted and the noise discarded by, for example, ensemble averaging. This signal

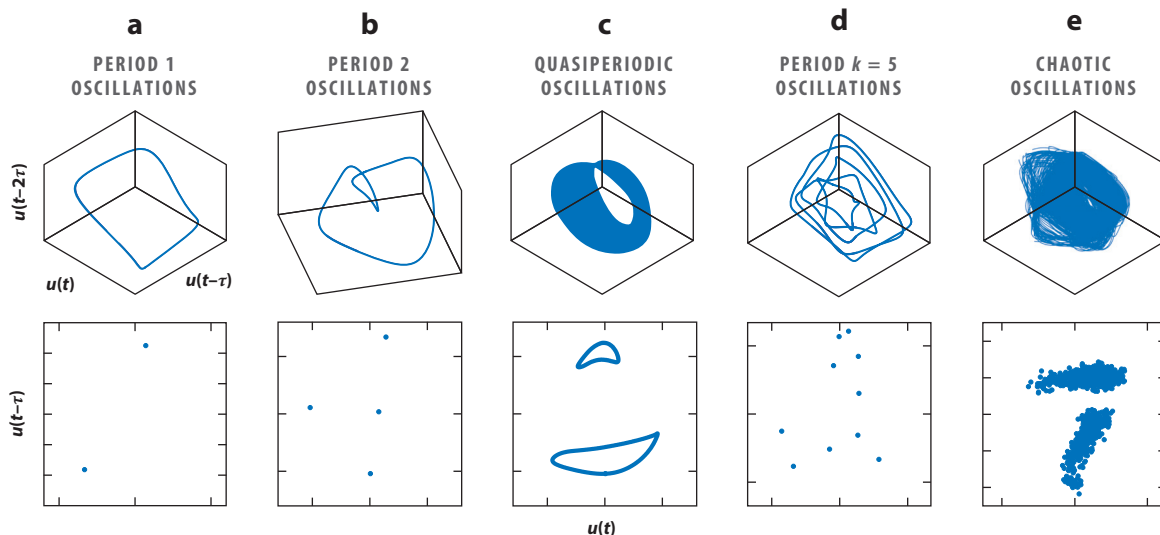


**Figure 9**

Numerical simulations showing phase portraits and Poincaré sections of the acoustic velocity at the flame,  $u_f$ , for different types of self-excited oscillations of a two-dimensional slot-stabilized premixed flame in a duct. The images depict (a) period 1 oscillations, (b) period 2 oscillations, (c) quasiperiodic oscillations, (d) period  $k = 5$  oscillations, and (e) chaotic oscillations. Adapted from Kashinath et al. (2014, figure 10).

plus noise paradigm is useful (Section 4.1), but tools from dynamical systems and complex systems theory (Section 4.2) provide further insight because the discarded fluctuations, which are caused by the complex nonlinear interaction between the acoustic field and turbulent flow, contain information with diagnostic and prognostic value.

#### 4.1. Stochastic Approach

In turbulent combustors, the thermoacoustically stable state is characterized by combustion noise, which is generated by turbulent reacting flow, has broadband characteristics, and is often assumed to be stochastic (Clavin et al. 1994, Burnley & Culick 2000, Lieuwen 2002). Lieuwen & Banaszuk (2005) considered noise to be forcing of the dynamical system (additive noise) or fluctuation of the system's parameters (parametric noise). Clavin et al. (1994) studied turbulence-induced noise in high-frequency thermoacoustic oscillations with stochastic differential equations. They modeled the influence of turbulence on the heat release rate as parametric noise by assuming that the turbulent fluctuations are slower than the acoustic fluctuations. This noise appears as a multiplicative noise term in their wave equation. Their Fokker-Planck equation for the evolution of the transition probability density function for the amplitude of oscillations predicts erratic bursts, as observed in experiments.

Noiray & Schuermans (2013a) and Noiray & Denisov (2017) modeled combustion noise as additive white noise and analyzed supercritical bifurcations with stochastic differential equations. They extracted linear quantities, such as the growth rate, using output-only model-based system identification of noisy pressure measurements, validating their methodology with simulations (Noiray 2017). By measuring chemiluminescence, they disentangled the growth rate due to thermoacoustics from the decay rate due to acoustic damping (Boujo et al. 2016). This stochastic

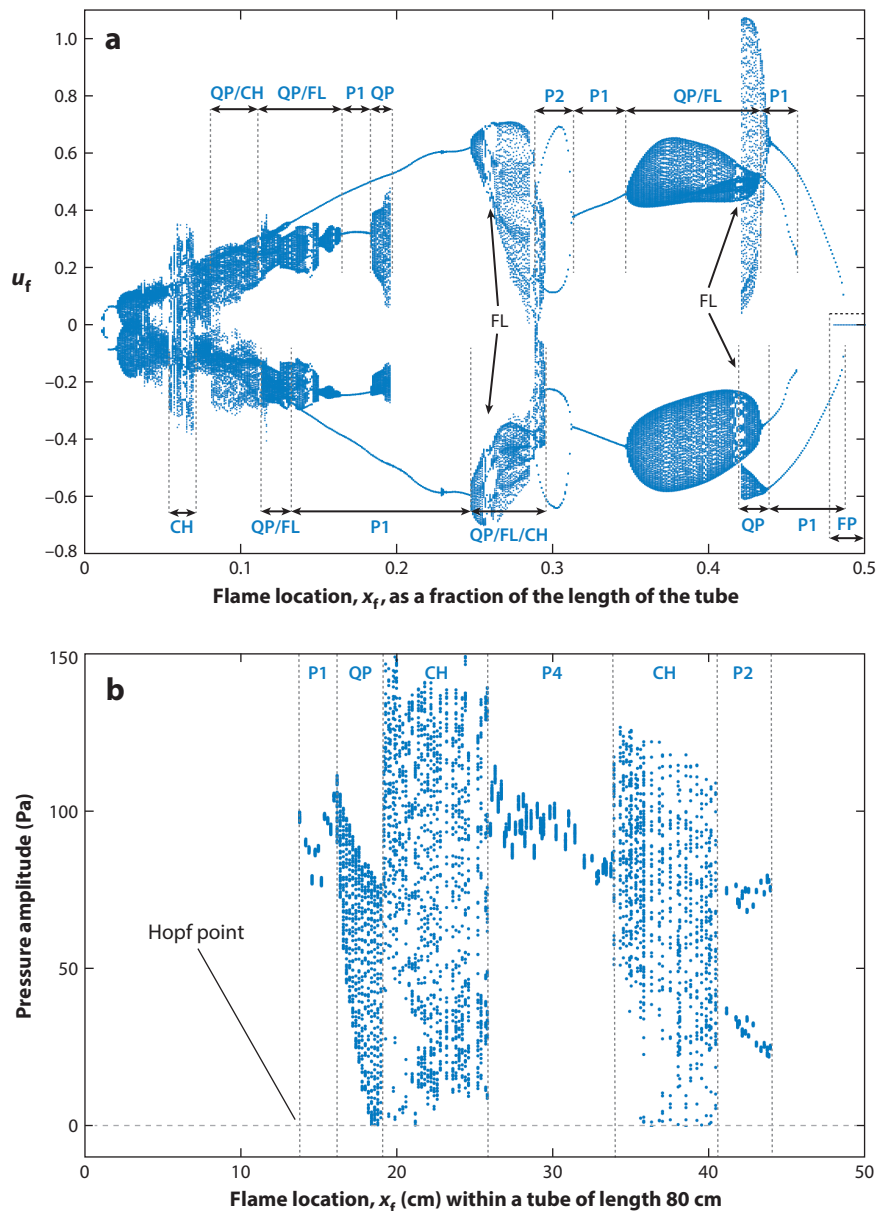


**Figure 10**

(a) Peak values of the acoustic velocity,  $u_f$ , as a function of flame position,  $x_f$ , for numerical simulations of a two-dimensional slot-stabilized premixed flame in a duct with two open ends. There are abrupt changes in behavior at certain values of  $x_f$  and multiple possible solutions at other values. Adapted from Kashinath et al. (2014). (b) Peak values of the acoustic pressure as a function of flame position,  $x_f$ , for experiments on an array of seven premixed conical flames in a duct with one open end and one closed end. There are abrupt changes in behavior at certain values of  $x_f$ . Adapted from Kabiraj et al. (2012a). Abbreviations: CH, chaotic; FL, frequency-locked; P1, period 1; P2, period 2; P4, period 4; QP, quasiperiodic.

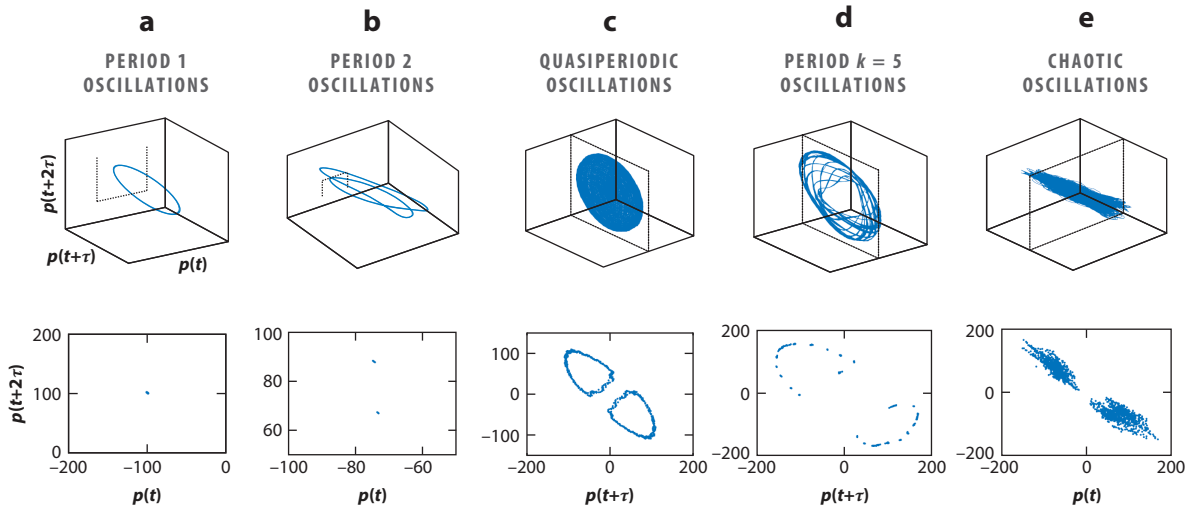


**Figure 11**

Experimentally determined phase portraits (*top*) and Poincaré sections (*bottom*) for self-excited oscillations of a hexagonal array of seven premixed conical flames in a duct: (a) period 1, (b) period 2, (c) quasiperiodic, (d) period  $k$ , and (e) chaotic. Figure reproduced from Kabiraj et al. (2012b, figure 4).

approach explains the intermittent switching between spinning and standing modes in annular combustion chambers (Noiray & Schuermans 2013b).

This analysis is also applicable to subcritical bifurcations, although the bistable region reduces as the noise increases. This can be seen by averaging the results of many numerical simulations (Waugh & Juniper 2011), by experimental observation (Gopalakrishnan & Sujith 2015), and by integrating the stochastic governing equations (Tony et al. 2015). Tony et al. (2015) showed that the bistable region is completely suppressed at high noise amplitudes.

## 4.2. Deterministic Approach

Combustion noise is not always stochastic. Gotoda et al. (2012), for example, experimentally examined thermoacoustic behavior close to lean blowout, where the dynamics are dominated by stochastic fluctuations. As the equivalence ratio increases, the behavior transitions to low-dimensional chaotic oscillations, then to periodic oscillations, then to quasiperiodic oscillations (Gotoda et al. 2015), and then back to chaotic oscillations. Kabiraj et al. (2015b) experimentally investigated noise-induced dynamics just before the bistable region of a laminar flame thermoacoustic system with a subcritical Hopf bifurcation. They found noisy precursors as they approached the bifurcation and attributed them to coherence resonance, which is noise-induced enhancement of deterministic dynamics in a nonlinear system. These noise-excited oscillations are irregular for low and high noise amplitudes but coherent for moderate amplitudes (Pikovskiy & Kurths 1997).

**4.2.1. Intermittency.** In turbulent combustors, the onset of thermoacoustic oscillation is preceded by intermittent bursts of high-amplitude periodic oscillations amidst a background of low-amplitude aperiodic fluctuations (Nair et al. 2014) (**Figure 12**). These intermittent bursts last longer as the point of onset is approached and are also reported in other studies (Clavin et al. 1994, Gotoda et al. 2014, Huang 2015, Kabiraj et al. 2015a, Pawar et al. 2016, Wilhite et al. 2016). Intermittency is often analyzed using recurrence plots (**Figure 13**; see also **Supplemental**

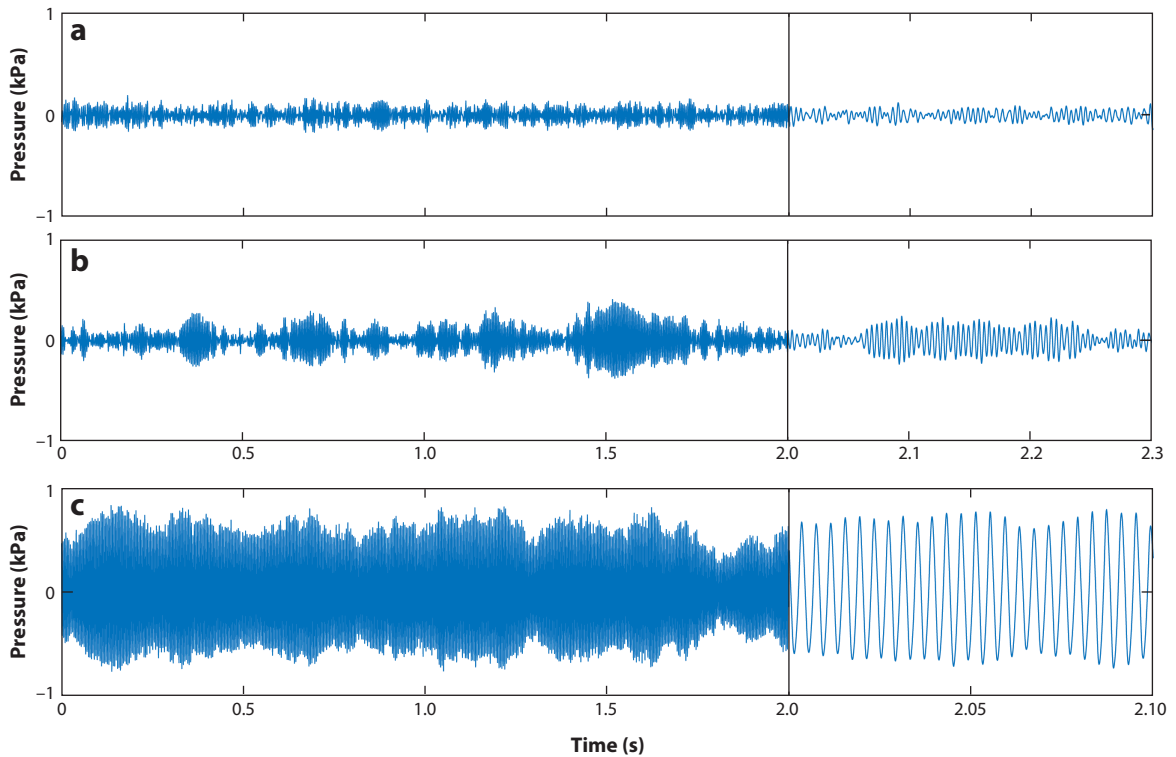


**Figure 12**

Pressure signals during (a) combustion noise (equivalence ratio  $\phi = 0.98$ ), where the signal is low amplitude and aperiodic; (b) intermittency ( $\phi = 0.76$ ), where oscillatory bursts appear randomly within an aperiodic signal; and (c) thermoacoustic oscillation ( $\phi = 0.69$ ), where the signal is periodic.

**Tutorial 2**, section 5), which represent time-series data graphically. Recurrence quantification analysis is used to obtain precursor measures, such as recurrence rate, trapping time, and Shannon entropy, to provide early warning of thermoacoustic instability. As thermoacoustic instability is approached, intermittent bursts arise when a hydrodynamic mode frequency is close to a duct acoustic frequency (Nair & Sujith 2015, Sampath & Chakravarthy 2016). Unni & Sujith (2017) showed that, during these intermittent bursts, the otherwise aperiodic flame rolls up periodically due to vortex shedding at the dump plane. Nair & Sujith (2015) developed a phenomenological model that qualitatively reproduces the intermittent bursts and transition to thermoacoustic oscillation for turbulent bluff body combustors. Mondal et al. (2017) examined the phase between heat release rate and acoustic pressure. They showed that, as expected, the acoustic pressure and heat release rate fluctuations are asynchronous during combustion noise, whereas they are synchronous during thermoacoustic instability. They also showed that, during intermittency, patches of synchronous and asynchronous motion coexist in the reaction zone, which is known as a chimera state (Abrams & Strogatz 2004).

**4.2.2. High-dimensional chaos, Hurst exponents, and multifractality.** Tony et al. (2015) performed determinism tests on turbulent combustors and showed that combustion noise has the features of high-dimensional chaos contaminated with white and colored noise. High-dimensional chaos transitions to periodic motion during the onset of thermoacoustic instability (Nair et al.

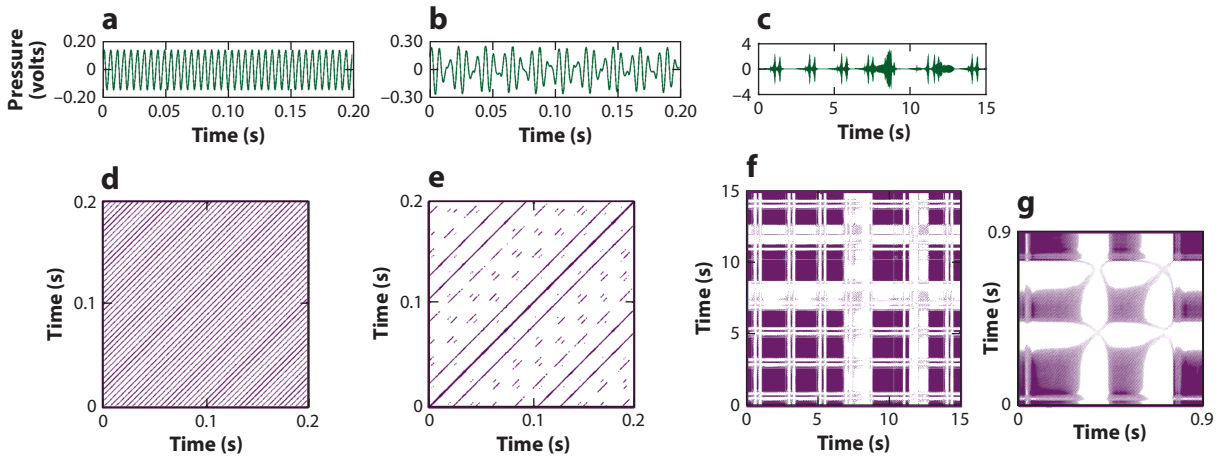


**Figure 13**

Time series (*a–c*) and recurrence plots (*d–g*) of pressure signals from a turbulent combustor. The state of a system can be represented as a point in  $n$ -dimensional phase space. In the recurrence plots, a coordinate  $(t_1, t_2)$  is colored purple if the system's state at time  $t_2$  is within a distance  $\epsilon$  of the system's state at time  $t_1$ . This shows (*a,d*) equally spaced diagonal lines for periodic oscillations, (*b,e*) separated diagonal lines for quasiperiodic oscillations, and (*c,f,g*) a checkered pattern for intermittent oscillations (see **Supplemental Tutorial 2**, section 5). Adapted from Kabiraj & Sujith (2012, figures 6 and 7).

**Supplemental Material**

2013). The time series for combustion noise is self-similar and can be analyzed with fractals. For a fractal series  $v(t)$  with fractal dimension  $D$ , the signal  $v(ct) = v(t)/c^H$  has the same statistics, where  $H = 2 - D$  is the Hurst exponent (West et al. 2003). Nair & Sujith (2014) showed that, as a system approaches thermoacoustic instability,  $H$  drops toward zero long before the oscillation amplitude rises (**Figure 14a,b**).

Fluctuations with different amplitudes can have different scaling behavior. Such time series are called multifractal and cannot be described by a single  $H$  (Mandelbrot 1999). This requires generalized Hurst exponents,  $H_q$ , which indicate the scaling behavior of the  $q$ -th central moments of

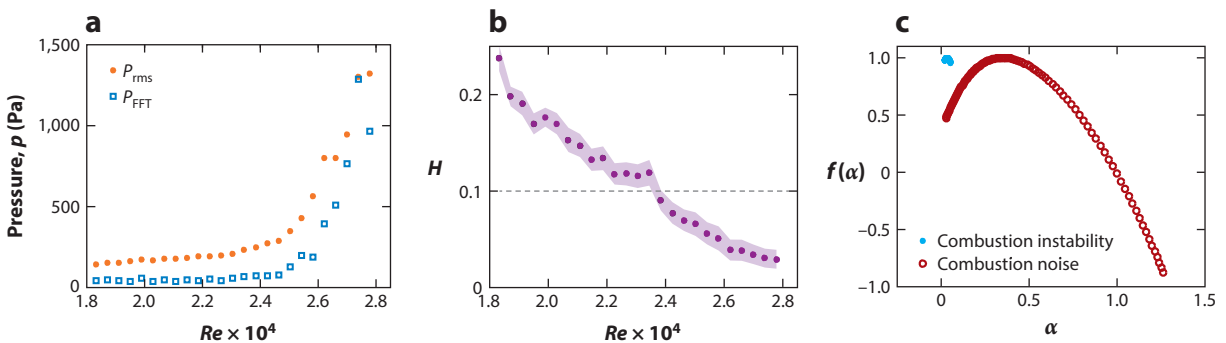


**Figure 14**

(*a*) Root mean square ( $p_{\text{rms}}$ ) and peak fast Fourier transform ( $p_{\text{FFT}}$ ) for pressure fluctuations in a turbulent combustor. (*b*) The Hurst exponent,  $H$ , with error range corresponding to six standard deviations. The Hurst exponent tends towards zero, indicating order arising from chaos, long before thermoacoustic oscillations reach appreciable amplitudes around  $Re = 2.4 \times 10^4$ . The dashed line at  $H = 0.1$  is an arbitrary but useful transition threshold. (*c*) Spectrum of singularities,  $f(\alpha)$ , for multifractal combustion noise, which has a wide spectrum, and combustion instability, which has a concentrated spectrum. Adapted from Nair & Sujith (2014, figure 7).

## REPRESENTING COMPLEX SYSTEMS USING COMPLEX NETWORKS

A complex system contains multiple interacting components, resulting in nontrivial and nonlinear collective behavior that cannot be discerned by studying the behavior of its individual components. A complex system is often analyzed by constructing a complex network that represents its connectivity patterns. The characteristics of the network topology are studied using measures from graph theory. Scale-free networks have a heavy-tailed distribution of connectivity with no characteristic scales (Barabási & Albert 1999). Many real-world networks, such as the Internet, scientific collaboration networks, protein networks, and power grids, exhibit the characteristics of a scale-free network.

the time series. For a monofractal signal,  $H_q$  is the same for different values of  $q$ . For a multifractal signal,  $H_q$  is different for different values of  $q$ . Through a Legendre transformation, this variation of  $H_q$  can be represented as a spectrum of singularities  $f(\alpha)$ , where  $\alpha$  is the conjugate variable corresponding to  $q$  (Kantelhardt 2012) (**Figure 14c**). The width of the singularity spectrum gives the degree of multifractality in the signal. Unni & Sujith (2015) used the Hurst exponent and Unni (2016) used recurrence quantification to detect the onset of thermoacoustic instability and lean blowout in turbulent combustors, describing the two phenomena within the same framework rather than separately as a dynamic instability (thermoacoustic) and a static instability (blowout).

**4.2.3. Complex networks to study thermoacoustic instability.** Combustion systems operate over a wide range of scales, from molecular mixing, to turbulent transport, to large-scale acoustic waves. This complex interaction leads to rich dynamics, with multifractal chaotic fluctuations (combustion noise) on the one hand and periodic oscillations (thermoacoustic instability) on the other. Complexity, which arises from the large number of interacting elements, is a characteristic of many physical and biological systems (see **Supplemental Tutorial 2**, section 6).

Complex networks (see the sidebar titled Representing Complex Systems Using Complex Networks) have been used to understand the dynamics underlying time-series data (Lacasa et al. 2008, Donner et al. 2010). In thermoacoustics, Murugesan & Sujith (2015) used complex networks to investigate the scale invariance of combustion noise by applying a visibility algorithm (Lacasa et al. 2008) to time-series data from turbulent combustors. They showed that the complex networks obtained from combustion noise can be represented as a scale-free network (Barabási & Albert 1999). The power-law distributions of connections in the scale-free network are related to the scale invariance of combustion noise. Furthermore, they showed that, during the transition to combustion instability, the scale-free feature of combustion noise disappears, and order emerges in the complex network topology. Okuno et al. (2015) used complex networks to show that pseudoperiodicity and high dimensionality exist in the dynamics of thermoacoustic instability, including the possible presence of a clear power-law distribution and small-world-like nature. Precursors for thermoacoustic instability (Murugesan & Sujith 2016) can be devised through the statistical theory of complex networks (Lesne & Lagues 2011). Finally, the most sensitive points in the network (Yu et al. 2009) might be identified, aiding effective passive control.

 [Supplemental Material](#)

### SUMMARY POINTS

1. Rocket and gas turbine combustion chambers have high volumetric heat release rates and low acoustic damping. Thermoacoustic oscillations arise if the efficiency of the thermoacoustic mechanism is even slightly positive for one or more acoustic modes.

2. The efficiency of the thermoacoustic mechanism is sensitive to many parameters, in particular the time delay between an acoustic perturbation at the fuel injector and a subsequent heat release rate perturbation at the flame. In turn, these parameters are sensitive to changes in the engine's design and operating point and to environmental conditions.
3. This extreme sensitivity allows thermoacoustic systems to be stabilized with small design changes, usually at the full engine test stage. The challenge is to devise and implement these design changes cheaply, quickly, and early in the design process.
4. Most nonlinear analyses assume that thermoacoustic oscillations are periodic, with harmonic acoustics. Continuation methods show, however, that these oscillations are rarely harmonic and, furthermore, are often unstable to period doubling or quasiperiodic motion. Numerical simulations and experiments confirm this and reveal period 2, period  $k$ , quasiperiodic, and chaotic motion. This nonlinear behavior causes strong sensitivity to parameters.
5. Quantities such as the linear growth rate can be extracted from a stochastic analysis of experimental measurements of turbulent thermoacoustic systems. This analysis also explains the observed bursts of erratic amplitude evolution.
6. If turbulent fluctuations are treated deterministically with dynamical systems theory, then thermoacoustic oscillations can be considered as order emerging from chaos via intermittent bursts of periodic oscillations.
7. A time series corresponding to combustion noise has multifractal characteristics and can be represented by a scale-free complex network. At the onset of thermoacoustic instability, multifractality disappears, and the complex network becomes regular. Measures based on multifractality, complex networks, and intermittency statistics provide useful early warning signs for thermoacoustic instability.

## FUTURE ISSUES

1. In most thermoacoustic systems, there are many design parameters but only a few unstable modes. Adjoint methods are therefore ideal for identifying small design changes that stabilize these modes. However, they require an accurate model of the system.
2. Devising accurate thermoacoustic models is challenging because extreme sensitivity to parameters introduces considerable systematic error if parameters cannot be estimated accurately. One solution is to calculate parameters from automated experimental measurements and inverse uncertainty quantification. Parameters learned on laboratory-scale rigs can then be updated as tests are performed on larger-scale rigs.
3. For nonlinear behavior, the FDF will remain a useful tool. An FDF, once measured, can be combined with any acoustic network to predict stable or unstable limit cycles. The next challenge is to apply this to industrial configurations, either with strong actuation in experiments or by creating accurate FDFs with CFD.
4. Continuation methods are less restrictive than FDF methods and may eventually replace them. They are more expensive than the FDF if a given flame is to be examined within many different acoustic networks but are cheaper for a single acoustic network.

5. The signal plus noise paradigm will remain useful, for example, to infer linear growth rates from noisy data. It will be complemented by tools from dynamical systems theory and complex systems theory.
6. The temporal and spatiotemporal dynamics of the onset of thermoacoustic instability can be studied with complex systems theory. Temporal analysis of acoustic pressure measurements can be performed in real time and provides early warning signs of impending thermoacoustic instability. Spatiotemporal analysis provides more detail but requires quantitative diagnostic techniques such as high-speed chemiluminescence imaging of methylidyne (CH) or hydroxyl (OH) radicals, in conjunction with simultaneous acoustic pressure measurements.
7. Complex systems theory can also be applied to self-excited turbulent thermoacoustic systems simulated with high-fidelity large-eddy simulations.
8. Concepts from nonlinear dynamics and complex systems theory could reveal the nature of coupling among flow, combustion, and acoustic fields. Identifying and exploiting the most sensitive points in this network will improve passive control methods.

## DISCLOSURE STATEMENT

The authors are not aware of any biases that might be perceived as affecting the objectivity of this review.

## ACKNOWLEDGMENTS

We would like to thank Sébastien Candel, Swetaprovo Chaudhuri, Hiroshi Gotoda, Tim Lieuwen, Luca Magri, Jonas Moeck, Vineeth Nair, Franck Nicoud, Nicolas Noiray, and Santosh Shanbhogue for their comments on the original manuscript and the European Research Council (ALORS 2590620), the Department of Science and Technology (DST), and the Office of Naval Research Global (ONRG) for their financial support.

## LITERATURE CITED

- Abrams DM, Strogatz SH. 2004. Chimera states for coupled oscillators. *Phys. Rev. Lett.* 93:174102
- Ananthakrishnan N, Deo S, Culick FEC. 2005. Reduced-order modeling and dynamics of nonlinear acoustic waves in a combustion chamber. *Combust. Sci. Technol.* 177:221–48
- Armitage C, Balachandran R, Mastorakos E, Cant R. 2006. Investigation of the nonlinear response of turbulent premixed flames to imposed inlet velocity oscillations. *Combust. Flame* 146:419–36
- Bade S, Wagner M, Hirsch C, Sattelmayer T, Schuermans B. 2013. Design for thermo-acoustic stability: procedure and database. *J. Eng. Gas Turbines Power* 135:121507
- Balachandran R, Ayoola BO, Kaminski CF, Dowling AP, Mastorakos E. 2005. Experimental investigation of the nonlinear response of turbulent premixed flames to imposed inlet velocity oscillations. *Combust. Flame* 143:37–55
- Balasubramanian K, Sujith RI. 2008. Thermoacoustic instability in a Rijke tube: non-normality and nonlinearity. *Phys. Fluids* 20:044103
- Barabási AL, Albert R. 1999. Emergence of scaling in random networks. *Science* 286:509–12
- Bauerheim M, Nicoud F, Poinso T. 2016. Progress in analytical methods to predict and control azimuthal combustion instability modes in annular chambers. *Phys. Fluids* 28:021303

- Bellows BD, Bobba MK, Forte A, Seitzman JM, Lieuwen T. 2007. Flame transfer function saturation mechanisms in a swirl-stabilized combustor. *Proc. Combust. Inst.* 31:3081–88
- Bellucci V, Flohr P, Paschereit CO, Magni F. 2004. On the use of Helmholtz resonators for damping acoustic pulsations in industrial gas turbines. *J. Eng. Gas Turbines Power* 126:271–75
- Boujo E, Denisov A, Schuermans B, Noiray N. 2016. Quantifying acoustic damping using flame chemiluminescence. *J. Fluid Mech.* 808:245–57
- Bourgouin JF, Durox D, Moeck J, Schuller T, Candel SM. 2015. Characterization and modeling of a spinning thermoacoustic instability in an annular combustor equipped with multiple matrix injectors. *J. Eng. Gas Turbines Power* 137:021503
- Burnley VS, Culick FEC. 2000. Influence of random excitations on acoustic instabilities in combustion chambers. *ALAA J.* 38:1403–10
- Candel SM. 1992. Combustion instabilities coupled by pressure waves and their active control. *Symp. Int. Combust.* 24:1277–96
- Candel SM. 2002. Combustion dynamics and control: progress and challenges. *Proc. Combust. Inst.* 29:1–28
- Candel SM, Durox D, Schuller T, Bourgouin JF, Moeck JP. 2014. Dynamics of swirling flames. *Annu. Rev. Fluid Mech.* 46:147–73
- Chomaz JM. 1993. Linear and non-linear, local and global stability analysis of open flows. In *Turbulence in Spatially Extended Systems*, ed. R Benzi, C Basdevant, S Ciliberto, pp. 245–57. Commack, NY: Nova Sci. Publ.
- Chomaz JM. 2005. Global instabilities in spatially developing flows: non-normality and nonlinearity. *Annu. Rev. Fluid Mech.* 37:357–92
- Chu BT. 1965. On the energy transfer to small disturbances in fluid flow (part I). *Acta Mech.* 1:215–34
- Clavin P, Kim JS, Williams FA. 1994. Turbulence-induced noise effects on high frequency combustion instabilities. *Combust. Sci. Technol.* 96:61–84
- Ćosić B, Moeck JP, Paschereit CO. 2014. Nonlinear instability analysis for partially premixed swirl flames. *Combust. Sci. Technol.* 186:713–36
- Crocco L. 1951. Aspects of combustion stability in liquid propellant rocket motors, part I: fundamentals. Low frequency instability with monopropellants. *J. Am. Rocket Soc.* 8:163–78
- Crocco L. 1969. Research on combustion instability in liquid propellant rockets. *Symp. Int. Combust.* 12:85–99
- Crocco L, Cheng SI. 1956. *Theory of Combustion Instability in Liquid Propellant Rocket Motors*. London: Butterworths
- Culick FEC. 1971. Non-linear growth and limiting amplitude of acoustic oscillations in combustion chambers. *Combust. Sci. Technol.* 3:1–16
- Culick FEC. 2006. *Unsteady motions in combustion chambers for propulsion systems*. RTO AGARDograph AG-AVT-039, Res. Technol. Organ., North Atl. Treaty Organ., Washington, DC
- Donner RV, Zou Y, Donges JF, Marwan N, Kurths J. 2010. Recurrence networks—a novel paradigm for nonlinear time series analysis. *New J. Phys.* 12:033025
- Dowling AP. 1997. Nonlinear self-excited oscillations of a ducted flame. *J. Fluid Mech.* 346:271–90
- Dowling AP. 1999. A kinematic model of a ducted flame. *J. Fluid Mech.* 394:51–72
- Dowling AP, Morgans AS. 2005. Feedback control of combustion oscillations. *Annu. Rev. Fluid Mech.* 37:151–82
- Dranovsky ML. 2007. *Combustion Instabilities in Liquid Rocket Engines: Testing and Development Practices in Russia*. Reston, VA: AIAA
- Ducruix S, Schuller T, Durox D, Candel S. 2003. Combustion dynamics and instabilities: elementary coupling and driving mechanisms. *J. Propuls. Power* 19:722–34
- Durox D, Schuller T, Noiray N, Candel S. 2009. Experimental analysis of nonlinear flame transfer functions for different flame geometries. *Proc. Combust. Inst.* 32:1391–98
- Eldredge JD, Dowling AP. 2003. The absorption of axial acoustic waves by a perforated liner with bias flow. *J. Fluid Mech.* 485:307–35
- Gelb A, Vander Velde WE. 1968. *Multiple-Input Describing Functions and Nonlinear System Design*. New York: McGraw-Hill
- Gopalakrishnan EA, Sujith RI. 2015. Effect of external noise on the hysteresis characteristics of a thermoacoustic system. *J. Fluid Mech.* 776:334–53

- Gotoda H, Amano M, Miyano T, Ikawa T, Maki K, Tachibana S. 2012. Characterization of complexities in combustion instability in a lean premixed gas-turbine model combustor. *Chaos* 22:043128
- Gotoda H, Nikimoto H, Miyano T, Tachibana S. 2011. Dynamic properties of combustion instability in a lean premixed gas-turbine combustor. *Chaos* 21:013124
- Gotoda H, Okuno Y, Hayashi K, Tachibana S. 2015. Characterization of degeneration process in combustion instability based on dynamical systems theory. *Phys. Rev. E* 92:052906
- Gotoda H, Shinoda Y, Kobayashi M, Okuno Y, Tachibana S. 2014. Detection and control of combustion instability based on the concept of dynamical system theory. *Phys. Rev. E* 89:022910
- Gysling DL, Copeland GS, McCormick DC, Proscia WM. 2000. Combustion system damping augmentation with Helmholtz resonators. *J. Eng. Gas Turbines Power* 122:269–74
- Han X, Li J, Morgans AS. 2015. Prediction of combustion instability limit cycle oscillations by combining flame describing function simulations with a thermoacoustic network model. *Combust. Flame* 162:3632–47
- Harrje DT, Reardon FH. 1972. *Liquid propellant rocket combustion instability*. Tech. Rep. NASA-SP-194, Natl. Aeronaut. Space Admin., Washington, DC
- Heckl M. 1990. Non-linear acoustic effect in the Rijke tube. *Acoustica* 72:63–71
- Hemchandra S. 2012. Premixed flame response to equivalence ratio fluctuations: comparison between reduced order modeling and detailed computations. *Combust. Flame* 159:3530–43
- Higgins B. 1802. On the sound produced by a current of hydrogen gas passing through a tube. *J. Nat. Philos. Chem. Arts* 1:129–31
- Hill DC. 1992. *A theoretical approach for analyzing the restabilization of wakes*. Tech. Rep. 103858, Natl. Aeronaut. Space Admin., Washington, DC
- Hill DC. 1995. Adjoint systems and their role in the receptivity problem for boundary layers. *J. Fluid Mech.* 292:183–204
- Huang Y. 2015. *Advanced methods for validating combustion instability predictions using pressure measurements*. PhD Thesis, Purdue Univ., West Lafayette, IN
- Huang Y, Yang V. 2009. Dynamics and stability of lean-premixed swirl-stabilized combustion. *Prog. Energy Combust. Sci.* 35:293–364
- Jahnke CC, Culick FEC. 1994. Application of dynamical systems theory to nonlinear combustion instabilities. *J. Propuls. Power* 10:508–17
- Jegadeesan V, Sujith RI. 2013. Experimental investigation of noise induced triggering in thermoacoustic systems. *Proc. Combust. Inst.* 34:3175–83
- Juniper MP. 2011. Triggering in the Rijke tube: non-normality, transient growth and bypass transition. *J. Fluid Mech.* 667:272–308
- Juniper MP. 2012. Triggering in thermoacoustics. *Int. J. Spray Combust. Dyn.* 4:217–38
- Kabiraj L, Saurabh A, Karimi N, Sailor A, Mastorakos E, et al. 2015a. Chaos in an imperfectly premixed model combustor. *Chaos* 25:023101
- Kabiraj L, Saurabh A, Wahi P, Sujith RI. 2012a. Route to chaos for combustion instability in ducted laminar premixed flames. *Chaos* 22:023129
- Kabiraj L, Steinert R, Saurabh A, Paschereit CO. 2015b. Coherence resonance in a thermoacoustic system. *Phys. Rev. E* 92:042909
- Kabiraj L, Sujith RI. 2012. Nonlinear self-excited thermoacoustic oscillations: intermittency and flame blowout. *J. Fluid Mech.* 713:376–97
- Kabiraj L, Sujith RI, Wahi P. 2012b. Bifurcations of self-excited ducted laminar premixed flames. *J. Eng. Gas Turbines Power* 134:31502
- Kantelhardt JW. 2012. Fractal and multifractal time series. In *Mathematics of Complexity and Dynamical Systems*, ed. RA Meyers, pp. 463–87. Berlin: Springer
- Karimi N, Brear MJ, Jin SH, Monty JP. 2009. Linear and non-linear forced response of a conical, ducted, laminar premixed flame. *Combust. Flame* 156:2201–12
- Kashinath K, Waugh IC, Juniper MP. 2014. Nonlinear self-excited thermoacoustic oscillations of a ducted premixed flame: bifurcations and routes to chaos. *J. Fluid Mech.* 761:399–430
- Kerswell RR. 2018. Nonlinear nonmodal stability theory. *Annu. Rev. Fluid Mech.* 50:319–45
- Kim KT, Lee JG, Quay BD, Santavicca DA. 2010a. Response of partially premixed flames to acoustic velocity and equivalence ratio perturbations. *Combust. Flame* 157:1731–44

- Kim KT, Lee JG, Quay BD, Santavicca DA. 2010b. Spatially distributed flame transfer functions for predicting combustion dynamics in lean premixed gas turbine combustors. *Combust. Flame* 157:1718–30
- Komarek T, Polifke W. 2010. Impact of swirl fluctuations on the flame response of a perfectly premixed swirl burner. *J. Eng. Gas Turbines Power* 132:061503
- Krediet HJ, Beck CH, Krebs W, Schimek S, Paschereit CO, Kok JBW. 2012. Identification of the flame describing function of a premixed swirl flame from LES. *Combust. Sci. Technol.* 184:888–900
- Lacasa L, Luque B, Ballesteros F, Luque J, Nun JC. 2008. From time series to complex networks: the visibility graph. *PNAS* 105:4972–75
- Landau LD. 1944. On the problem of turbulence. *C. R. Acad. Sci. URSS* 44:387–91
- Lesne A, Lagues M. 2011. *Scale Invariance: From Phase Transitions to Turbulence*. Berlin: Springer
- Lieuwen TC. 2002. Experimental investigation of limit-cycle oscillations in an unstable gas turbine combustor. *J. Propuls. Power* 18:61–67
- Lieuwen TC. 2012. *Unsteady Combustor Physics*. Cambridge, UK: Cambridge Univ. Press
- Lieuwen TC, Banaszuk A. 2005. Background noise effects on combustor stability. *J. Propuls. Power* 21:25–31
- Lieuwen TC, McManus KR. 2003. Introduction: combustion dynamics in lean-premixed prevaporized (LPP) gas turbines. *J. Propuls. Power* 19:721
- Lieuwen TC, Yang V. 2005. *Combustion Instabilities in Gas Turbine Engines: Operational Experience, Fundamental Mechanisms, and Modeling*. Reston, VA: AIAA
- Luchini P, Bottaro A. 2014. Adjoint equations in stability analysis. *Annu. Rev. Fluid Mech.* 46:493–517
- Macquisten MA, Whiteman M, Stow SR, Moran AJ. 2014. Exploitation of measured flame transfer functions for a two-phase lean fuel injector to predict thermoacoustic modes in full annular combustors. *Proc. ASME Turbo Expo, Düsseldorf, Ger., June 16–20*, Pap. GT2014-25036. New York: Am. Soc. Mech. Eng.
- Magri L, Bauerheim M, Juniper MP. 2016a. Stability analysis of thermo-acoustic nonlinear eigenproblems in annular combustors. Part I. Sensitivity. *J. Comput. Phys.* 325:395–410
- Magri L, Bauerheim M, Nicoud F, Juniper MP. 2016b. Stability analysis of thermo-acoustic nonlinear eigenproblems in annular combustors. Part II. Uncertainty quantification. *J. Comput. Phys.* 325:411–21
- Magri L, Juniper MP. 2013. Sensitivity analysis of a time-delayed thermo-acoustic system via an adjoint-based approach. *J. Fluid Mech.* 719:183–202
- Magri L, Juniper MP. 2014. Global modes, receptivity, and sensitivity analysis of diffusion flames coupled with duct acoustics. *J. Fluid Mech.* 752:237–65
- Mandelbrot BB. 1999. *Multifractals and Noise: Wild Self-Affinity in Physics*. Berlin: Springer
- Matveev KI. 2003a. Energy consideration of the nonlinear effects in a Rijke tube. *J. Fluids Struct.* 18:783–94
- Matveev KI. 2003b. *Thermoacoustic instabilities in the Rijke tube: experiments and modeling*. PhD Thesis, Calif. Inst. Technol., Pasadena
- McManus KR, Poinso T, Candel SM. 1993. A review of active control of combustion instabilities. *Prog. Energy Combust. Sci.* 19:1–29
- Mensah GA, Moeck JP. 2017. Acoustic damper placement and tuning for annular combustors: an adjoint-based optimization study. *J. Eng. Gas Turbines Power* 139:061501
- Moeck JP, Bothein MR, Schimek S, Lacarelle A, Paschereit CO. 2008. *Subcritical thermoacoustic instabilities in a premixed combustor*. Presented at 14th AIAA/CEAS Aeroacoust. Conf., May 5–7, Vancouver, AIAA Pap. 2008–2946
- Mondal S, Unni VR, Sujith RI. 2017. Onset of thermoacoustic instability in turbulent combustors: an emergence of synchronized periodicity through formation of chimera-like states. *J. Fluid Mech.* 811:659–81
- Mongia HC, Held TJ, Hsiao GC, Pandalai RP. 2003. Challenges and progress in controlling dynamics in gas turbine combustors. *J. Propuls. Power* 19:822–29
- Murugesan M, Sujith RI. 2015. Combustion noise is scale-free: transition from scale-free to order at the onset of thermoacoustic instability. *J. Fluid Mech.* 772:225–45
- Murugesan M, Sujith RI. 2016. Detecting the onset of an impending thermoacoustic instability using complex networks. *J. Propuls. Power* 32:707–12
- Nair V, Sujith RI. 2014. Multifractality in combustion noise: predicting an impending combustion instability. *J. Fluid Mech.* 747:635–55
- Nair V, Sujith RI. 2015. A reduced-order model for the onset of combustion instability: physical mechanisms for intermittency and precursors. *Proc. Combust. Inst.* 35:3193–200

- Nair V, Thampi G, Karuppusamy S, Gopalan S, Sujith RI. 2013. Loss of chaos in combustion noise as a precursor of impending combustion instability. *Int. J. Spray Combust. Dyn.* 5:273–90
- Nair V, Thampi G, Sujith RI. 2014. Intermittency route to thermoacoustic instability in turbulent combustors. *J. Fluid Mech.* 756:470–87
- Nicoud F, Benoit L, Sensiau C, Poinso T. 2007. Acoustic modes in combustors with complex impedances and multidimensional active flames. *ALAA J.* 45:426–41
- Nicoud F, Wieczorek K. 2009. About the zero Mach number assumption in the calculation of thermoacoustic instabilities. *Int. J. Spray Combust. Dyn.* 1:67–111
- Noiray N. 2017. Linear growth rate estimation from dynamics and statistics of acoustic signal envelope in turbulent combustors. *J. Eng. Gas Turbines Power* 139:041503
- Noiray N, Denisov A. 2017. A method to identify thermoacoustic growth rates in combustion chambers from dynamic pressure time series. *Proc. Combust. Inst.* 36:3843–50
- Noiray N, Durox D, Schuller T, Candel S. 2008. A unified framework for nonlinear combustion instability analysis based on the flame describing function. *J. Fluid Mech.* 615:139–67
- Noiray N, Durox D, Schuller T, Candel S. 2009. Dynamic phase converter for passive control of combustion instabilities. *Proc. Combust. Inst.* 32:3163–70
- Noiray N, Schuermans B. 2013a. Deterministic quantities characterizing noise driven Hopf bifurcations in gas turbine combustors. *Int. J. Non-Linear Mech.* 50:152–63
- Noiray N, Schuermans B. 2013b. On the dynamic nature of azimuthal thermoacoustic modes in annular gas turbine combustion chambers. *Proc. R. Soc. Lond.* 469:20120535
- Oberleithner K, Schimek S, Paschereit CO. 2015. Shear flow instabilities in swirl-stabilized combustors and their impact on the amplitude dependent flame response: a linear stability analysis. *Combust. Flame* 162:86–99
- O'Connor J, Acharya V, Lieuwen T. 2015. Transverse combustion instabilities: acoustic, fluid mechanic, and flame processes. *Prog. Energy Combust. Sci.* 49:1–39
- Oefelein JC, Yang V. 1993. Comprehensive review of liquid-propellant combustion instabilities in F-1 engines. *J. Propuls. Power* 9:657–77
- Okuno Y, Small M, Gotoda H. 2015. Dynamics of self-excited thermoacoustic instability in a combustion system: pseudo-periodic and high-dimensional nature. *Chaos* 25:043107
- Orchini A, Rigas G, Juniper MP. 2016. Weakly nonlinear analysis of thermoacoustic bifurcations in the Rijke tube. *J. Fluid Mech.* 805:523–50
- Palies P, Durox D, Schuller T, Candel S. 2011. Nonlinear combustion instability analysis based on the flame describing function applied to turbulent premixed swirling flames. *Combust. Flame* 158:1980–91
- Paschereit CO, Schuermans B, Polifke W, Mattson O. 2002. Measurement of transfer matrices and source terms of premixed flames. *J. Eng. Gas Turbines Power* 124:239–47
- Pawar SA, Vishnu R, Vadivukkarasan M, Panchagnula MV, Sujith RI. 2016. Intermittency route to combustion instability in a laboratory spray combustor. *J. Eng. Gas Turbines Power* 138:041505
- Pikovsky AS, Kurths J. 1997. Coherence resonance in a noise-driven excitable system. *Phys. Rev. Lett.* 78:775–78
- Poinso T. 2017. Prediction and control of combustion instabilities in real engines. *Proc. Combust. Inst.* 36:1–28
- Poinso TJ, Trouvé AC, Veynante DP, Candel SM. 1987. Vortex-driven acoustically coupled combustion instabilities. *J. Fluid Mech.* 177:265–92
- Prieur K, Durox D, Schuller T, Candel S. 2016. *The describing function of swirled spray flames*. Presented at 24th Int. Congr. Theor. Appl. Mech., Aug. 21–26, Montreal
- Provansal M, Mathis C, Boyer L. 1987. Bénard–von Kármán instability: transient and forced regimes. *J. Fluid Mech.* 182:1–22
- Rankine WJM. 1870. On the thermodynamic theory of waves of finite longitudinal disturbance. *Proc. R. Soc. Lond.* 18:80–83
- Rayleigh JWSB. 1878. The explanation of certain acoustical phenomena. *Nature* 18:319–21
- Rayleigh JWSB. 1896. *The Theory of Sound*, Vol. 2. New York: Dover
- Reynolds WC, Hussain AKMF. 1972. The mechanics of an organized wave in turbulent shear flow. Part 3. Theoretical models and comparisons with experiments. *J. Fluid Mech.* 54:263–88

- Richards G, Straub DL, Robey EH. 2003. Passive control of combustion dynamics in stationary gas turbines. *J. Propuls. Power* 19:795–810
- Rigas G, Jamieson NP, Li LKB, Juniper MP. 2016. Experimental sensitivity analysis and control of thermoacoustic systems. *J. Fluid Mech.* 787:R1
- Sampath R, Chakravarthy SR. 2016. Investigation of intermittent oscillations in a premixed dump combustor using time-resolved particle image velocimetry. *Combust. Flame* 172:309–25
- Schimke S, Moek JP, Paschereit CO. 2011. An experimental investigation of the nonlinear response of an atmospheric swirl-stabilized premixed flame. *J. Eng. Gas Turbines Power* 133:101502
- Schmid PJ. 2007. Nonmodal stability theory. *Annu. Rev. Fluid Mech.* 39:129–62
- Schmid PJ, Henningson D. 2001. *Stability and Transition in Shear Flows*. Berlin: Springer
- Shreekrishna, Hemchandra S, Lieuwen TC. 2010. Premixed flame response to equivalence ratio perturbations. *Combust. Theory Model.* 14:681–714
- Sipp D, Lebedev A. 2007. Global stability of base and mean flows: a general approach and its applications to cylinder and open cavity flows. *J. Fluid Mech.* 593:333–58
- Sirignano WA. 2016. Driving mechanisms for combustion instability. *Combust. Sci. Technol.* 187:162–205
- Sondhauss C. 1850. Über die Schallschwingungen der Luft in erhitzten Glasröhren und in gedeckten Pfeifen von ungleicher Weite. *Ann. Phys. Chem.* 79:1–34
- Steele RC, Cowell LH, Cannon SM, Smith CE. 2000. Passive control of combustion instability in lean premixed combustors. *J. Eng. Gas Turbines Power* 122:412–19
- Sterling JD, Zukoski EE. 1991. Nonlinear dynamics of laboratory combustor pressure oscillations. *Combust. Sci. Technol.* 77:225–38
- Strogatz S. 1994. *Nonlinear Dynamics and Chaos*. Boulder, CO: Westview Press
- Subramanian P, Mariappan S, Sujith RI, Wahi P. 2010. Bifurcation analysis of thermoacoustic instability in a horizontal Rijke tube. *Int. J. Spray Combust. Dyn.* 2:325–55
- Subramanian P, Sujith RI, Wahi P. 2013. Subcritical bifurcation and bistability in thermoacoustic systems. *J. Fluid Mech.* 715:210–38
- Suchorsky MK, Sah SM, Rand RH. 2010. Using delay to quench undesirable vibrations. *Nonlinear Dyn.* 62:407–16
- Summerfield M. 1951. A theory of unstable combustion in liquid propellant rocket systems. *J. Am. Rocket Soc.* 21:108–14
- Tammisola O, Juniper MP. 2016. Coherent structures in a swirl injector at  $Re = 4800$  by nonlinear simulations and linear global modes. *J. Fluid Mech.* 792:620–57
- Tony J, Gopalakrishnan EA, Sreelekha E, Sujith RI. 2015. Detecting deterministic nature of pressure measurements from a turbulent combustor. *Phys. Rev. E* 92:062902
- Truffin K, Poinsot T. 2005. Comparison and extension of methods for acoustic identification of burners. *Combust. Flame* 142:388–400
- Unni VR. 2016. *A unified approach to study lean blowout and thermoacoustic instability*. PhD Thesis, Indian Inst. Technol. Madras, Chennai, India
- Unni VR, Sujith RI. 2015. Multifractal characteristics of combustor dynamics close to lean blowout. *J. Fluid Mech.* 784:30–50
- Unni VR, Sujith RI. 2017. Flame dynamics during intermittency in a turbulent combustor. *Proc. Combust. Inst.* 36:3791–98
- Vishnu R, Sujith RI, Aghalayam P. 2015. Role of flame dynamics on the bifurcation characteristics of a ducted V-flame. *Combust. Sci. Technol.* 187:894–905
- Waugh I, Illingworth S, Juniper MP. 2013. Matrix-free continuation of limit cycles for bifurcation analysis of large thermoacoustic systems. *J. Comput. Phys.* 240:225–47
- Waugh IC, Juniper MP. 2011. Triggering in a thermoacoustic system with stochastic noise. *Int. J. Spray Combust. Dyn.* 3:225–42
- Waugh IC, Kashinath K, Juniper MP. 2014. Matrix-free continuation of limit cycles and their bifurcations for a ducted premixed flame. *J. Fluid Mech.* 759:1–27
- West BJ, Latka M, Glaubic-Latka M, Latka D. 2003. Multifractality of cerebral blood flow. *Physica A* 318:453–60

- Willhite J, Dolan B, Villalva Gomez R, Kabiraj L, Paschereit CO, Gutmark E. 2016. *Analysis of combustion oscillations in a staged MLDI burner using decomposition methods and recurrence analysis*. Presented at AIAA SciTech Forum Expo., Jan. 8–12, Gaylord Palms, FL, AIAA Pap. 2016-1156
- Worth NA, Dawson JR. 2013. Modal dynamics of self-excited azimuthal instabilities in an annular combustion chamber. *Combust. Flame* 160:2476–89
- Yi T, Santavicca DA. 2010. Flame transfer functions for liquid-fueled swirl-stabilized turbulent lean direct fuel injection combustion. *J. Eng. Gas Turbines Power* 132:021506
- Yu W, Chen G, Lü J. 2009. On pinning synchronization of complex dynamical networks. *Automatica* 45:429–35
- Zhu M, Dowling AP, Bray KNC. 2002. Forced oscillations in combustors with spray atomizers. *J. Eng. Gas Turbines Power* 124:20–30
- Zinn B. 1970. A theoretical study of non-linear damping by Helmholtz resonators. *J. Sound Vib.* 13:347–56
- Zinn BT, Lores ME. 1971. Application of the Galerkin method in the solution of non-linear axial combustion instability problems in liquid rockets. *Combust. Sci. Technol.* 4:269–78